

This is a repository copy of Short length-scale variability of hybrid event beds and its applied significance.

White Rose Research Online URL for this paper: <a href="https://eprints.whiterose.ac.uk/id/eprint/87008/">https://eprints.whiterose.ac.uk/id/eprint/87008/</a>

Version: Accepted Version

#### Article:

Fonnesu, M, Haughton, P, Felletti, F et al. (1 more author) (2015) Short length-scale variability of hybrid event beds and its applied significance. Marine and Petroleum Geology, 67. pp. 583-603. ISSN: 1873-4073

https://doi.org/10.1016/j.marpetgeo.2015.03.028

# Reuse

Items deposited in White Rose Research Online are protected by copyright, with all rights reserved unless indicated otherwise. They may be downloaded and/or printed for private study, or other acts as permitted by national copyright laws. The publisher or other rights holders may allow further reproduction and re-use of the full text version. This is indicated by the licence information on the White Rose Research Online record for the item.

#### **Takedown**

If you consider content in White Rose Research Online to be in breach of UK law, please notify us by emailing eprints@whiterose.ac.uk including the URL of the record and the reason for the withdrawal request.



# SHORT LENGTH-SCALE VARIABILITY OF HYBRID EVENT BEDS AND ITS APPLIED

**SIGNIFICANCE** 

Marco Fonnesu <sup>a\*</sup>, Peter Haughton <sup>a</sup>, Fabrizio Felletti <sup>b</sup> and William McCaffrey <sup>c</sup>

<sup>a</sup> UCD School of Geological Sciences, University College of Dublin, Belfield, Dublin 4, Ireland

<sup>b</sup> Dipartimento di Scienze della Terra, Università degli Studi di Milano, Via Mangiagalli 34, 20034 Milano,

Italy

<sup>c</sup> Turbidite Research Group, School of Earth Sciences, University of Leeds, Leeds LS2 9JT, UK

Keywords: Sediment gravity flow, Turbidites, Hybrid event beds, Lateral variability, Linked-debrites,

Reservoir quality

\* = Corresponding author: M. Fonnesu (<u>marco.fonnesu@ucdconnect.ie</u>)

# Abstract

Hybrid event beds (HEBs) are a type of deep-water sediment gravity flow deposit that generally comprise a basal clean sandstone overlain by a variety of muddier and less-permeable sandy facies. They are thought to be emplaced by combinations of turbidity currents, transitional flows and debris flows, all as part of the same transport event. To date, a number of studies have highlighted the common presence of HEBs mainly in the outer and marginal parts of deep-water systems where they replace beds composed dominantly of clean sand up-dip and/or axially over scales of km to 10s km. In addition to these broad patterns, important yet poorly understood short-length facies changes (over metres to 100s m) occur, modifying the overall texture and reservoir characteristics at or beneath typical spacing of production wells. The nature and origin of the short length-scale transitions is here addressed in four well-exposed HEB-prone outcrops: the Cretaceous-Paleocene Gottero Sandstone and the Miocene Cilento Flysch, both in Italy, the Carboniferous Mam Tor Sandstone in northern England, and the Carboniferous basal Ross Sandstone Formation, Western Ireland. A series of detailed correlation panels show marked lateral variations in internal bed make-up for most of the hybrid event beds studied. This variability typically involves lateral changes in the proportions of the cleaner basal sandstone and the overlying muddy sandstone division that occur without substantial change in the overall event bed thickness. The variability is inferred to reflect the complex fingering between the up-dip sandstone-dominated part of the event bed and the down-dip linked debrite due to internal erosion (ploughing) of the debrite into the basal clean sand. Where the upper part of the bed is dominated by large mudstone rafts, these may have foundered into liquefied sand and been injected and partly fragmented by the sand intrusions. The variable thickness and continuity of the basal clean sandstones have important implications for reservoir characterisation; significant variability in bed character at interwell scale can be anticipated. Rugose contacts between the intra-bed facies divisions may impact on drainage and sweep efficiency during hydrocarbon production.

# 1. INTRODUCTION

Sandstones deposited by turbidity currents are an important component of many hydrocarbon reservoirs (Nilsen et al., 2007). These largely turbulent flows can progressively fractionate their sediment load, leaving graded deposits that are at least moderately well sorted with most of the clay segregated to form mudstone units (the T<sub>e</sub> division; Bouma 1962) capping relatively porous and permeable sandstone beds. However, many reservoirs also include, or in some cases are dominated by, stacked event beds comprising a basal clean (i.e. clay-poor) sandstone division overlain by a variety of muddier and less permeable sandy facies. These hybrid event beds (*sensu* Haughton et al., 2009) are thought to form from flows that were at least partly turbulent, but that also had zones of damped turbulence beneath or from which clay and sand were emplaced together by linked debris flows and/or transitional flows (*sensu* Baas et al. 2009, 2011). Consequently the reservoir properties of much of the sandy part of the event bed are compromised by high matrix-clay concentrations (Fugelli and Olsen, 2007). In addition, the significant lateral extent of the muddy sand component means that the cleaner and better quality sandstones in the basal part of stacked event beds are poorly connected, particularly vertically. Amy et al. (2009) have used sector models to show that once the muddy sand component of a hybrid event bed exceeds c. 20%, the facies make-up has a significant impact on production efficiency in terms of volumes of oil produced and more rapid water breakthrough.

The term hybrid event bed (HEB) was introduced (Haughton et al. 2009) to describe a common bed motif in deep-water successions occurring alongside more familiar turbidity current deposits (turbidites). The designation builds on the earlier concept of linked debrites (Haughton et al., 2003) and incorporates the slurry flow ideas developed by Lowe and Guy (2000). An ideal five-part structure was identified (Fig.1A) comprising (from base to top) a basal, generally graded, structureless sandstone (termed H1) in some cases

with scattered mudclasts (H1b), a unit of banded sandstone comprising alternating cleaner/paler sands loaded into darker argillaceous sandstone bands (H2), a chaotic division of argillaceous sandstone with variable concentrations of mudstone clasts and sheared sand patches (H3), a fine/very fine grained, parallel- and ripple-laminated sandstone (H4) and a silty mudstone capping division (H5). All divisions are not always present in the one bed (Haughton et al., 2010; Talling, 2013). H1 thins at the expense of H3 and pinches out distally and laterally. The H2 division may be absent, or subtle and easily overlooked; in other cases it is greatly expanded and can dominate the deposit such as in the margins of the Lower Cretaceous Britannia sandstone beds (Barker et al., 2008). H4 may be absent or may wholly or partly have collapsed into the underlying H3 division. Event beds broadly conforming to the hybrid model have been widely documented in cores from hydrocarbon wells (Haughton et al., 2003, 2009; Barker et al., 2008; Davis et al., 2009; Kane and Ponten, 2012), shallow sea floor cores (Zeng et al., 1991; Talling et al., 2007b; Georgiopoulou et al., 2009; Lee et al., 2013) and outcrops (Wood and Smith, 1959; Mutti et al., 1978; Van Vliet, 1978; Ricci Lucchi and Valmori, 1980; Sylvester and Lowe, 2004; Talling et al., 2004; 2007a; 2012; Amy and Talling, 2006; Ito, 2008; Hodgson, 2009; Jackson et al., 2009; Muzzi Magalhaes and Tinterri, 2010; Tinterri and Muzzi Magalhaes; 2011).

A number of mechanisms have been proposed to explain the development of hybrid event beds and the emplacement of the argillaceous sands/sandstones they contain. The variable structure and range of contexts in which they occur suggest they can form in more than one way. Key to most of the mechanisms is an active role for clay in damping turbulence and modulating the flow behaviour (Baas and Best, 2002). Where the models differ is in the emphasis put on vertical as opposed to lateral changes in flow structure and rheology. Baas et al. (2009, 2011) characterised the structure of transitional clay-rich flows in open channels showing progressive turbulence modulation and emphasising top-down onset of plug-flow with modified (enhanced and then damped) turbulent flow beneath before it is eventually extinguished. Sumner et al. (2009) used experimental data to show progressive turbulence damping in rapidly decelerating clay-rich flows with sand initially settling from a turbulence-modified suspension to form the H1 division before the suspension stiffens to leave an overlying poorly graded argillaceous sand or sandy mud (a fluid mud emplacing H3). Kane and Ponten (2012) applied a similar model to deep-water sandstones in the Gulf of Mexico, stressing the role of vertical rheological heterogeneity in what were inferred to be transitional flows with turbulent

basal layers and overlying quasi-laminar layers. The common presence of micas, clay chips and carbonaceous fragments in many H3 divisions, indicating prior hydraulic fractionation of components, is important. In these cases, efficient longitudinal and transverse segregation of components with lower settling velocities (see Pyles et al., 2013) into slower moving sectors of the flow may then force transformations, triggering the onset of transitional and then quasi-laminar flow conditions. The character of the aggrading deposit can therefore sample different sectors of the flow as it passes, with clean sand (H1) deposited from the still turbulent flow front and increasingly argillaceous sand (H2 and H3) from further back in the flow. Large and far-travelled flows may have significant sectors with transitional characteristics, explaining instances of very thick banded (H2) divisions such as those in the Britannia Sandstone Formation (Lowe and Guy, 2000; Barker et al., 2008). Many H3 divisions include volumetrically significant mudstone clasts and this suggests a link between the onset of HEB deposition and up-dip erosion. In these cases, part of the flow is enriched in mudclasts which then disintegrate to release clays near bed that then modify the flow structure. Terlaky and Arnott (2014) infer that matrix-rich sandstones resembling hybrid event beds in the Windermere Group occur in the margins of plane-wall jets or hydraulic jumps linked to near-by channel avulsions. In this case, clay and mudstone clasts were suspended by local erosion and moved to adjacent lower energy flow sectors where they were deposited as poorly sorted and matrix-rich sandstones. A last mechanism involves partial transformation of a debris flow to a turbidity current up-dip, with remnants of the debris flow continuing to travel basinwards behind the head of the forerunning turbidity current. The trailing H4/5 division in all cases is inferred to represent a dilute wake suspended by shearing from the head and upper surface of the main flow.

A common general observation is that hybrid event beds become increasingly important in the outer and marginal parts of many systems where they replace beds composed dominantly of clean sand either up-dip and/or axially (Haughton et al., 2003; Hodgson, 2009). In several cases, the internal character of the bed changes laterally despite a relatively constant thickness (Davis et al., 2009). The nature of these transitions, which are expressed at length scales of kms to 10s kms, has largely been inferred on the basis of detailed correlation of widely spaced (kms apart) outcrop sections (Amy and Talling, 2006; Talling et al., 2012; Hodgson, 2009; Muzzi Magalhaes and Tinterri, 2010), seabed cores (Talling et al., 2007b; Lee et al., 2013) or wells (Haughton et al., 2003; Davis et al., 2009), or by using vertical bed successions to infer lateral

relationships using Walther's Law (Kane and Ponten, 2012). These studies have demonstrated that transitions between turbidites and hybrid event beds can occur either progressively over long distances (many kms) or over shorter length-scales (a km or so; Hodgson, 2009, Patacci et al., 2014), and that the debritic component of the bed (H3 division of Haughton et al. 2009) may occur on the fringe of, or in some cases centrally within the wider deposit (Fig. 1B-E). Shorter length-scale (km) transitions from turbidite to hybrid event bed are particularly common where flows are forced to decelerate against topography (Muzzi Magalhaes and Tinterri, 2010; Patacci et al., 2014) or where they expand rapidly forming plane-wall jets (Terlaky and Arnott 2014). More subtle basin floor topography can be important in either triggering or delaying linked debrite formation and may contribute to more complex patterns of debrite distribution, including local pods of debrite developed in zones of flow expansion or lower gradient that promote flow transformation (Talling et al., 2007b; Davis et al., 2009).

These spatial changes in bed make-up (i.e., facies tracts) provide a useful predictive tool for lithology and by implication net-reservoir trends in HEB - prone systems. However, they can be overprinted by significant variability at much shorter length scales (10-100s m) that are less well understood and not particularly well captured by long distance correlations between widely separated sites. This variability typically involves lateral changes in the proportions of cleaner H1 sandstone and H3 muddy sandstone at a scale of 10s to 100s m, particularly in beds where H2 is poorly developed and where the H3 division is charged with mudstone clasts. This kind of lateral variability was implicit in the linked debrite model (Haughton et al., 2003) and has been documented by Hodgson (2009) who reported irregular H1/H3 boundaries in clast-rich hybrid event beds in the Tanqua Karoo fan systems. Such short length scale variations were interpreted by Talling (2013) to result from erosion of the sandstone by the linked H3 debrite but, in spite of a close link between the turbidity current and debris flow, it was unclear how a similar overall bed thickness could be maintained despite spatially-variable internal erosion. Significantly, variable relative proportions of H1 and H3 can be present in the absence of local sea floor topography and in these cases it cannot relate to local adjustments of the flow to gradient change and flow non-uniformity (cf. Patacci et al. 2014). Such variability is important, because it can impact on how event beds are correlated between nearby wells; such beds may have a rather different vertical expression despite being only a few hundred metres apart. Another consequence is the development of significant rugosity along the top of the clean sandstone component of the bed (in some cases even eroding it completely) which may impact on drainage and sweep efficiency during production in hydrocarbon reservoirs.

The aim of the study reported here is to describe, characterise and account for short length-scale lateral variability in a series of well-exposed hybrid event bed-prone successions: the Miocene San Mauro Formation in the Cilento Flysch and Cretaceous-Paleocene Gottero Sandstone, both in Italy, and two Carboniferous examples, the Mam Tor Sandstone in northern England, and the basal Ross Sandstone Formation, western Ireland (Fig. 2; Tab.1). The four examples are drawn from basins in a range of tectonic settings; thrust-top and trench-slope basins in the case of Cilento, and Gottero respectively, and post-rift basins in the case of Mam Tor and the Ross. The Italian field examples are the principal focus of this study and are treated in more detail; the other examples are used to confirm the bed transition types that are identified and to demonstrate that similar short-length scale variability is widely developed. The studies jointly inform a revised model for the geometry of hybrid event beds in the critical transition from up-dip turbidite to fringing hybrid event bed, incorporating small-scale lateral variability. In addition, the potential implications of such a model for hydrocarbon production in fan fringe successions are considered.

# 2. METHODOLOGY

All four study locations represent well-exposed outcrops of ancient deep sea successions. In the case of the Gottero, Cilento and Mam Tor sections, serial sedimentological logs have been measured bed by bed at 1:50 scale and spaced laterally at distances of a few metres to 10s metres m apart. The Ross example is documented using a photomosaic of an inaccessible cliff section. Beds were traced directly in the field by simply walking them out, or by using aerial photographs guided by key correlatable horizons such as particularly thick beds. Grain-size measurements were made using a hand lens and grain-size comparator and corroborated by selected thin section analysis; the Udden-Wentworth grain size scale is used throughout. The analysis was conducted at bed scale, but also incorporated textural and structural characteristics of the component facies ("depositional intervals", *sensu* Ghibaudo, 1992) and information on their arrangement within the event beds. An "event bed" can be thought of as the vertical expression at one location of the longitudinal flow structure (Kneller and McCaffrey, 2003) and preserves information on both lateral changes in flow properties and flow evolution. Bed amalgamation is rare in all the studied successions and thus

individual event beds are complete and easily distinguished. Bed and depositional interval thicknesses, the geometry of bed boundary surfaces, sedimentary structures and palaeocurrent indicators were all recorded.

The terms clean sandstone, mudstone clast-rich clean sandstone and muddy sandstone are used to distinguish specific lithologies in the field on the basis of colour, weathering pattern and degree of induration. Thinsections were cut from representative samples from Gottero (11 samples) and Mam Tor (3 samples) to characterise the clay distribution, volume and character (Fig. 3). The proportion of pore-filling detrital clay has been determined by point-counting (500 points) distinguished framework grains, mica flakes, organic material, compact or deformed mud chips and clay matrix. Those sandstones designated clean (whether with or without floating mudstone clasts) are yellow-brown or light grey in colour and framework grain-supported with relatively low (9-13%) interstitial detrital clay, although with mud chips and clay aggregates in sandstones containing larger mudstone blocks. Sandstones designated muddy are dark grey or grey-green in colour, fissile, recessively weathered and have grain interstices choked with clay (17-26%) but with framework sand grains that are still in contact. The muddy sandstones also have common mica flakes (average 12%). The fabrics are distinct from the matrix-rich sandstones described by Terlaky and Arnott (2014) which are very poorly sorted and have sand grains floating in an abundant clay matrix (30% to >50%).

#### 3. CASE STUDIES

# 3.1. Geological settings

The four case studies (Fig. 2) are drawn from a range of basin contexts but were chosen because they share some common characteristics in term of lateral facies trends. The Cretaceous-Paleocene Gottero Sandstone unit (Fig. 2A) represents a deep-sea fan system filling a confined trench-slope basin (Nilsen and Abbate, 1984; Marroni et al., 2004). This developed on ophiolitic crust and its associated sedimentary cover of the Ligurian-Piedemont Basin. The sandstones were sourced from the Sardinia-Corsica massif (Parea, 1964; Van de Kamp and Leake, 1995) and formed a small fan system with a radius estimated at between 30 and 50 km (Nilsen and Abbate, 1984). The beds studied here come from the uppermost part of the Gottero succession in the Mount Ramaceto area. This is interpreted as an outer fan succession (Abbate and Sagri, 1970; Casnedi,

1982; Nilsen and Abbate, 1984; Marini, 1994). The area underwent significant tectonic deformation during the Eocene and Oligocene as part of the Alpine accretionary wedge (Marroni et al., 2004). As a result, the Mount Ramaceto succession was inverted on the overturned limb of a regional syncline (Casnedi, 1982; Marroni, 1991; Marroni et al., 2004). However, stratal disruption was minimal and individual beds can be traced laterally across the outcrop with no evidence for structural discontinuities or internal bed disruption.

The Upper Carboniferous Mam Tor Sandstone in UK Central Pennine Basin (Fig. 2B) and the Ross Formation in the Clare Basin, western Ireland (Fig. 2C), record post-rift deposition in basins that inherited their morphology from a phase of earlier Lower Carboniferous rifting (Collison, 1988; Martinsen et al., 1995). The Mam Tor Sandstone is a relatively small, deep-water fan system, probably no longer than 24 km long (Allen, 1960; Walker, 1966), developed in trough fed directly by fluvial and deltaic systems located towards the north and northwest (Aitkenhead et al., 2002). The Mam Tor outcrop, where the study is focused, represents the outer-fan and fan-fringe portion of the system (Walker, 1966). The Ross Sandstone Formation is a trough-confined sandy turbidite system which prograded from west and southwest into the Clare Basin. The studied section is located 2 km north of Ballybunion (Co. Kerry) in the lowermost, and by implication outermost, part of the Ross Formation.

The Miocene San Mauro Formation (Fig. 2D) is part of the Cilento Group, a complex sandy deep-water system developed in a wedge-top basin above the highly deformed Ligurian accretionary-complex (*Internidi* units). The succession contains a number of large marly megabeds related to the collapse of marginal carbonate platforms (MT beds in Fig. 2D; Cieszkowski et al., 1995; Nardi et al., 2003; Cavuoto et al., 2007), and common olistostromes and debris flow deposits (Butler and McCaffrey, 2010). The system was sourced primarily with siliciclastic sediments derived from Calabrian basement (Mostardini and Merlini, 1986; Bonardi et al., 1988; Patacca and Scandone, 1989). The section described here is from the Lago area and corresponds to the topmost part of the San Mauro Formation which is part of an extensive sheet turbidite system (Cavuoto et al., 2007).

Taken together, the studied sections help constrain different aspects of lateral heterogeneity expressed at bed level. The Gottero Sandstone, the Mam Tor Sandstone and the Ross Formation examples capture across-flow short-length lateral variability (over distances of 1 to 10s metres) in hybrid event beds whereas the Cilento

flysch case study is relevant mainly to facies variations parallel to flow expressed over slightly larger distance (100s m).

# 3.2. Gottero Sandstone in the Mount Ramaceto section, north-western Italy

The extensive exposures of the Cretaceous-Paleocene Gottero Sandstone in the Mount Ramaceto area offer a rare opportunity to trace individual beds continuously for up to four km (Fig. 4). The entire Gottero succession in this area is 1075 m-thick. The upper 750 m consists of basinal shales with associated high-and low-density turbidites and an unusually high proportion of hybrid event beds (c. 60 % of the beds > 50 cm are of hybrid character; 346 HEBs in total). These were deposited on a relatively flat sea floor in an outer-fan or basin-plain setting as suggested by the regional depositional trends and the tabular, sheet-like bed geometry at kilometre scale (Nilsen and Abbate, 1984). Here, the focus is on documenting the character and lateral variability of four representative event beds; the features shown are typical of many of the hybrid event beds in the upper Gottero succession at Mount Ramaceto.

The four event beds have been walked out and logged at a spacing of either every five metres (for *Bed 9, 9.3* and *16.1*) or in single metre steps (*Bed 18.3*; Figs 5 and 6). The orientation of the panels can be considered broadly perpendicular to the palaeoflow with angles of 60 to 80 degrees between palaeocurrents indicators and the panel (Fig. 3B).

Bed 18.3 is one of the thinner event beds (Fig. 5A) and can be followed for more than 3.3 km across the panel. In the south (section A), it is a 90 cm thick, medium grained, graded clean sandstone with scattered mudstone clasts (10-15 cm across) at the top. The bed changes to a hybrid event bed laterally in the centre of the panel before thinning to a 35 cm-thick parallel and ripple laminated fine to very fine grained sandstone in the north (section H). Serial logging of the hybrid portion of the bed (Fig. 5A) over a distance of 130 m shows that this is a four-part event bed made up of a clean, medium-grained, structureless and ungraded sandstone basal division (H1 sensu Haughton et al., 2009), overlain by a dark-coloured, recessively weathered H3 muddy sandstone interval rich in small (< 5 cm) mudstone chips and mica flakes (Fig. 7A). Larger mudstone clasts are absent. The bed is capped by a fine-grained, laminated sandstone (H4) that grades upward into an 8 to 12 cm-thick silty mudstone cap (H5). The bed has a generally flat base and top, except for the presence of occasional basal grooves (average palaeoflow orientation towards 308° N) which results

in a constant overall thickness (average of 87 cm) but with significant internal variability in terms of the relative thickness of its component parts. The boundary between H1 and H3 is well defined as a sharp irregular contact ranging in elevation laterally at metre-scale from 7 to 48 cm above the base of the event bed. The variable H1 thickness is almost everywhere compensated by the thickening and thinning of the H3 division which varies in thickness from 84 to 33 cm.

The stratigraphically higher *Bed 16.1* (Fig. 5B) varies from 175 to 245 cm thick across the main panel over a distance of 2.5 km. It has a variable internal character, in places dominated by clean sandstone, in other sections having a well-developed H3 division. Unlike *Bed 18.3*, the overall pattern of variability is less systematic although the sections to the north tend to be sandier. The study focusses on a 290 m long section of the bed demonstrating short-distance lateral transitions from clean sandstone with isolated mudclasts to a 55 m wide lense or pod of muddy sandstone (H3) on the southernmost end of the detailed panel (Fig. 5B). The latter contains abundant mudstone clasts (up to 15 cm across) and very common mudstone chips. The boundary H1b and H3 is diffuse and occurs over a few metres laterally at the northern end of the lense. The transition involves an increase in the mudstone clast content and in the clay dispersed in the sandstone matrix (from 14.6% to 20.8%). The H3 division thickens rapidly to the south, reaching a maximum of c. 140 cm about 30 m from the southern outcrop limit where the basal H1 division tapers to a minimum of 75 cm. The basal sandstone increases its thickness again in the southernmost logs leaving the H3 muddy-sandstone as an isolated patch.

A similar trend is displayed by *Bed 9* (Fig. 6A) but the muddy sandstone is more patchily distributed over the 584 metres section along which the bed has been traced. The sandy part of *Bed 9* has an average thickness of 337 cm and this includes a 235 cm thick mudstone cap. The base is coarse-grained and slightly erosive as can be noted by the two thin sandy beds beneath it that are missing in places due to erosional downcutting (Fig. 6A). *Bed 9* has an overall tabular geometry with subtle irregularities in the thickness that may reflect differential compaction of the softer muddier sandstone compared to the harder sandstone. The bed is dominated by large and variably abundant mudstone clasts (between 5 and 30 cm across with occasional metre-size clasts) that are concentrated in the top of the basal sandstone of the bed. It preserves gradual lateral transitions between mudstone clast-rich but clean sandstone (H1b facies) and muddy sandstone with

mudstone clasts (H3). These transitions happen with a wavelength of between 100 and 150 m upon which are superimposed shorter—wavelength irregularities of subdued amplitude, giving the H1/H3 boundary a complex geometry. The difference between the H1 and H3 texture can be seen in Figures 7C and 7D and in the corresponding thin-sections displayed in Figures 7E and 7F; samples were collected from the sandstone between the mudclasts in the two divisions. The H3 muddy sandstone (Fig. 7F) shows a higher quantity of detrital and pore-filling clay (20.4%) and small mud chips whereas the cleaner sandstone (Fig. 7E) has 12.4% detrital clay. The muddy sandstone contains abundant detrital mica flakes (15.8%) that are preferentially concentrated over the upper part of the H3 division. The bed top is a well-structured, planar to wavy laminated, fine-grained, clean sandstone (H4), 30 to 60 cm thick, that grades upward into the thick silty mudstone cap. An irregular medium grained sandstone interval with scattered mudstone clasts (Fig. 7D) locally intervenes between the H3 and H4 divisions and in places can be seen to be connected by vertical sand-injections with the basal H1 sandy division. Otherwise the boundary between H3 and H4 appears broadly planar at outcrop scale with no evidence of downward loading of H4 into H3.

Bed 9.3 (Fig. 6B) averages 405 cm thick and is a mainly muddy hybrid event bed in which the H3 division contains large mudstone blocks, some of which contain thin and deformed sandstone beds. The larger blocks are 1.5 to 16.0 metres long and are encased in muddy sandstone with many smaller mudstone clasts (5 to 25 cm across; Fig. 7B). In this case the muddy sandstone has 17.6% detrital clay. The transition between the H1 coarse to medium grained, structureless sandstone and the H3 muddy sandstone is sharp and extremely irregular and it is cross-cut by several cm to m-thick dyke-shaped sand injections intruding into H3 that locally form sills along the H3/H4 boundary. The H1 sandstone takes the form of a wedge, thinning from south to north, where the H3 division contains higher concentrations of larger blocks. The H1/H3 boundary has an extremely irregular shape, varying in elevation from 5 to 150 cm above the base of the event bed, over a few metres laterally. Such short length-scale irregularity is strongly influenced by the location of the largest mudstone rafts, the base of which tend to occupy the lowest position in the event bed above the thinnest preservation of basal H1 sandstone. The uppermost H4 fine-grained and laminated division has a very irregular base and a flat top: it develops m-scale loading structures that adorn the H3/H4 surface with pods of H4 sometimes foundering completely into the H3 muddier division. This character seems to be present where the mud content of the H3 division is higher.

#### 3.3. Mam Tor Sandstones in the Pennine Basin, UK

The Carboniferous Mam Tor sandstones are well exposed in high cliffs on the eastern side of Mam Tor, near Castleton, in northern England (Fig. 2B). The exposed succession is 123 m thick and it contains abundant hybrid event beds (41 % of beds; 237 HEBs in total; Davis, 2012). These can be followed laterally in the basal part of succession for up to 64 m laterally in what is an oblique, across-flow transect (Fig. 8A). The main palaeoflow in the studied stratigraphic interval, obtained from groove and flute orientations, is towards 242° (Fig. 8B). The overall stacking pattern is a broadly tabular, in which the thicker event beds (> 40 cm) are easily correlated and do not show appreciable thickness changes across the outcrop, whereas the thinner beds tend to be less continuous. There are, however, some exceptions to this pattern. For example in log B6 (Fig. 8A), mudstone clast-rich sandstones in the upper part of Bed e appear thinner than in the nearby sections and not completely compensated by the thickening of the H1 underlying sandstone. The correlation panel (Fig. 8B; modified from Davis, 2012) shows the relevant thickness changes in the internal divisions of individual hybrid event beds. In general, the bed tracing reveals: i) very short-scale lateral changes over less than 5 m within the same event bed between clean, erosive based sandstone (detrital clay content 13%) and beds with well-developed muddy and mudclast-rich sandstone divisions (detrital clay content 20%) (Bed b of Panel A: Fig. 8); ii) internal textural variations within H3 divisions from very muddy (average detrital clay content c. 26%) to sandier texture (Bed c of panel B); and iii) rapid thickness changes in the H1 and H3 divisions (Beds a of Panel A, Beds d and e of panel B). The H1/H3 boundary can be either sharp or transitional: the former appears erosive as in Bed d of Panel B (Section B8) where H3 mudclast-rich sandstone cuts through a H2 banded division. More diffuse boundaries tend to occur where the H1 sandstone is thicker, whereas abrupt boundaries are more common when it is thinner. The H4 division is typically absent in these event beds with a direct contact between the H3 muddy debrite and the H5 mudstone cap. It appears that the H4 division in some examples may never have been deposited, but in others it may have been eroded by the overlying bed or could possibly have completely foundered into and mixed with the debrite.

# 3.4. Lowermost Ross Formation at Ballybunion, western Ireland

The basal cycle of deposition in the Ross Formation, western Ireland, crops out north of Ballybunion (Fig. 2 C) and is characterised by a number of isolated outsized (several m thick), sheet-like hybrid event beds

(Barker, 2005; Haughton et al., 2009, 2010). The studied section is about 34 m thick from the first sandstone bed thicker than 5 cm, which is taken as the base of the Ross Formation, to the first of the main condensed sections, the *H.Smithi* marine band (Hodson, 1954; Lien et al., 2003). It is dominantly muddy (>90%) but is punctuated by six thick sandy event beds, the lower three of which are shown Figure 9. These were previously interpreted as slumps by Pyles and Jennette (2009), but they are here considered as the deposits of infrequent highly-efficient hybrid flows that travelled along the axis of the basin (Barker, 2005). They have unusually coarse-grained and dewatered sandy bases, in comparison to the monotonous fine and very fine structureless sandstones that characterise the rest of the Ross Formation.

The basal Ross hybrid event beds show highly irregular and sharp contacts between the H1 basal sandstone and the overlying, muddier H3 division, the texture of which is dominated by large mudstone blocks and sandstone rafts several metres long, surrounded by a mudclast-rich muddy sandstone matrix. Changes in thickness of the H1 division are particularly evident in  $Beds\ a$  and c shown in Figure 9. The H1 division thickness varies from 100 cm to 10 cm thick over a distance of less than 15 m for  $Bed\ a$  transverse to flow (palaeoflow towards N70°), and a similar relationship is seen in  $Bed\ c$  (see Fig. 9). By way of contrast the base of  $Bed\ b$  looks thinner and more tabular except in the places where the H3 debrite contains large (1-2 m scale) folded mudstone blocks that occupy grooves beneath which the underlying sandstone has been completely removed. The muddy sandstones are associated with sand-injections that intrude from the underlying basal sand into the H3 division in a similar way to  $Bed\ 9.3$  from the Gottero Sandstone, The H3 division compensates for the irregularities at the top of the H1 division and is in turn capped by thin and tabular H4 division giving the bed a generally planar geometry at outcrop scale.

# 3.5. Cilento Flysch in the Lago section, southern Italy

The Lago section, located in the north-western sector of the Cilento flysch basin, near the town of Castellabate, exposes 280 m of the topmost part of the San Mauro Formation (Fig. 2D). The section exhibits a wide variety of different types of event bed, including common hybrid event beds (8% of beds, 62 HEBs in total) and turbidite sandstones deposited by both high- and low-density currents.

Two main logs have been measured; a continuous Log A along a dirt road high on the coastal cliff and a composite Log B, linking seven different sections measured along the base of the cliffs (Figs 10A-B).

Overlapping logged sections are spaced between 85 and 290 m apart and thus correspond roughly to the distances between production wells in a densely-drilled hydrocarbon field (Fig. 10C). Flutes, grooves and ripples provided 34 palaeocurrent measurements which show a preferential source from the north-west (mean direction towards of 115°) with a very low dispersion (Fig. 10A-B). The orientation of the correlation panel with respect to the mean palaeoflow direction ranges from -20 to +23 degrees with the majority of the bed transition data collected along a roughly flow-parallel orientation (Fig. 10D).

The outcrop shows a broadly sheet-like geometry with some thick and laterally continuous event beds that provide good correlation markers (Fig. 11A-B). The sheet-like geometry applies only to the main system architecture, and not to the medium and thin-bedded bed stacks that can pinch-out or change in thickness between the measured sections. In the absence of multi-bed slumping and given the overall coherence of the palaeocurrent indicators, the succession is interpreted as a series of outer fan, lobe aggradation and retreat cycles (Cavuoto et al., 2007; Valente et al., 2014) punctuated by several outsize events that periodically were able to smooth the sea-floor.

From the 517 event beds measured in the Lago section, 482 beds have been correlated with high confidence between the two sections. The bed correlations establish rapid down-dip changes in bed character and in particular in the thickness and clay content of the H3 divisions of the hybrid event beds. The lateral facies transitions have been quantified and are reported in Table 2 and Fig. 12. They highlight that of the 43 beds with a hybrid expression in at least one of the sections, 36% retain a similar hybrid character between the two sections. Of the remainder, the normal down-dip changes from mudstone clast-rich, clean turbidite sandstones to HEBs occurs in 14% of the cases and from HEBs to laminated low-density turbidites in 12%, mostly in cases where the up-current HEB is relatively thin and comprises a basal clean medium grained sandstone and a muddy, highly mixed sand with only few mudstone chips. Somewhat surprisingly, 38% of the HEBs show a downstream transition to clean sandstone turbidites or to mudstone clast-rich turbidites (MRBs).

Representative examples of lateral transitions involving hybrid event beds and beds rich in mudstone clasts are provided in Fig. 12. They fall into six common patterns:

- Variable abundances of mudstone clasts within the same bed (Fig. 12A). The mudstone clast distribution does not always follow a consistent pattern with respect to the palaeoflow; they can be more abundant in either the up-dip or down-dip sections. The mudstone clasts can be randomly dispersed in relatively clean turbidite sandstone (e.g., Fig. 11B) or they may occur in dense clusters in which the clasts are in contact (e.g., Fig. 11C, *Bed 26*) but within 100 m down-dip the latter can change to a clean sandstone bed.
- Downcurrent HEB development from clean sandstone beds over short distances (250 m maximum; Fig. 12B). The change in bed character can be transitional, with the sand becoming progressively enriched in clay as in *Bed 188*, or more abrupt, showing a sharp passage from clean sandstone to muddy sandstone, as in *Bed 68* (in this case with associated development of chaotic texture).
- Up-dip transition from HEBs and mudclast-rich or clean sandstone (Fig. 12C). The H3 division in *Bed* 130 has a chaotic texture up-dip then shows an abrupt down-dip transition into a clean sandstone without an overall change in bed thickness.
- HEBs with internal changes in the proportion of H1 and H3 that can be expressed both by thickening (*Bed 182*) or thinning (*Bed 109*) of the muddy sandstone in a down-dip direction (Fig. 12D).
- HEBs showing no appreciable difference in bed character between the two correlated sections (e.g. *Beds* 195 and 153; Fig. 12E).
- Pinch-out of the H3 division (in HEBs up to 60 cm thick; Figs. 11E, 12F) and change down-dip to thin, fine-grained, structured turbidite sandstone (e.g. *Beds 178* and *110*). The loss of the muddy sandstone occurs over a distance of less than 130 m.

A significant observation is that mudclast-rich turbidites can correlate either up-dip or down-dip to hybrid event beds, transforming over relatively short distances (less than 150 m), but with down flow transitions more common. Up-dip transitions are preferentially seen in thicker and coarser base beds and associated with mudclast-rich or with chaotic and injected texture H3 divisions.

#### 4. ORIGIN OF THE STUDIED HYBRID EVENT BEDS

Various mechanisms have been invoked to account for the structure of hybrid event beds (see introduction). The studied examples are characterised by clast-rich and relatively sandy H3 divisions with interstitial clay rather than matrix-supported textures. They also include beds in which clast-rich muddy sandstones pass laterally over 10s to 100s m into clean sandstones with isolated or nests of mudstone clasts, or into clean sandstones devoid of mudstone clasts. The H3 divisions show significant lateral heterogeneity and none have sand-speckled mudstones ("starry night" textures) associated with well-mixed and far-travelled debris flows (Barker, 2008; Eggenhuisen et al., 2010). Mechanisms involving either simultaneous triggering of turbidity currents and debris flows from proximal slopes or partial transformation of a debris flow to a turbidity current are therefore ruled out in these cases. This interpretation is consistent with the paucity of debris flows in the deposits of the associated sandier inner fan successions (Ross Formation, Mam Tor, Gottero; Lien et al., 2003; Walker, 1966; Nilsen and Abbate, 1984); the debris flows either would have to have bypassed these areas, or alternatively to have formed down-dip. The composition of the mudstone clasts resembles the basin floor mudstones and there is no evidence for an exotic slope source in any of the examples studied.

The common occurrence of abundant mudstone clasts and the subdued clay abundances within the H3 divisions in the studied cases imply that simple deceleration of clay-rich flows is unlikely. In the Gottero case, the thicker event beds (>2 m) also have thick associated mudstone caps suggesting these flows carried significant clay loads, but these were deposited after the emplacement of the H3 divisions, possibly from ponded suspensions given that they are of similar thickness to the sandy lower part of the bed. The decelerating experimental flows examined by Baas et al. (2011) were unable to separate clay and sand once the concentration of clay exceeded 12%, emplacing thick fluid mud layers (see also Sumner et al., 2009); the sandy mudstones that might be expected were clay-rich flows to have arrested in this manner are not seen in this study.

The abundant mudstone clasts and in some cases large (m-scale) mudstone rafts point to erosion and incorporation of substrate mud as the key factor influencing subsequent flow evolution (Mutti et al., 1978; Van Vliet, 1978; Haughton et al., 2003; Talling et al., 2004; Muzzi Magalhaes and Tinterri, 2010; Lee et al., 2013; Terkey and Arnott, 2014). The mud clasts could have been acquired by collapse of distal slopes that turbidity currents impinged on (Kneller and McCaffrey, 1999), but this is doubtful in that a potential nearby confining slope was only present in the Mam Tor case, and there the depositing flows had not yet reached it. Hence up-dip erosional entrainment of clay and mud clasts is the favoured mechanism to account for the

development of hybrid and mudstone clast-rich turbidite beds. Entrainment of clasts may occur at various points along the flow path prior to hybrid event bed deposition. It could arise from the erosion of an out-ofgrade slope some distance away (Haughton et al, 2009), possibly caused by synsedimentary thrusting or other tectonic forcing (Haughton et al, 2009, Tinterri and Muzzi Magalhaes, 2011), or from more local erosion, for example of the mounded tops of previously deposited lobe bodies (Mutti et al., 1977), or channel-lobe transition zones or avulsion nodes where there can be extensive scouring (Mutti and Normark 1987, Wynn et al. 2002; Terlaky and Arnott, 2014). The studied event beds are distinct from the matrix-rich and very poorly sorted beds described by Terlaky and Arnott (2014) that were attributed to deposition on the margins of plane-wall jets and hydraulic jump zones. The variable H3 texture suggests mud clasts and rafts incorporated in the flows were hydraulically separated and transported away from the site of entrainment to varying degrees; zones containing comminuted mud chips and abundant hydraulically separated mica flakes (e.g. Gottero Bed 18.3; many of the Mam Tor examples) probably travelled further than those containing large m-scale rafts with sand injections. Entrained mud clasts may have travelled as bedload, with clast abrasion and disintegration supplying chips and dispersed clays. These materials may have damped turbulence so as to have eventually produced a plug flow in which the remaining clasts were suspended. The poor development of H2 banded sandstones suggests transitional flow was relatively unimportant in the studied systems and that the mud clast - bearing part of the flows arrested rapidly. Alternatively, the entrained mud clasts and rafts may have been buried by a rapidly aggrading sand bed, and then driven as a shear layer beneath the overriding flow (Butler and Tavernelli, 2006). In this case, segregation of the mud clasts may have influenced the mechanical properties of the just-deposited bed rather the turbulence structure of the overriding flow. The evidence of mud entrainment provides the context within which the development of significant lateral heterogeneity at short length scales is explored further below.

## 5. LATERAL HETEROGENEITY IN HYBRID EVENT BEDS

The case studies described above highlight a variety of short distance (10s-100s m) lateral changes in the character of hybrid event beds in both dip and strike sections. Two types of intra-bed heterogeneity are identified: (1) beds in which the lenticular H3 mudclast-rich muddy sandstone divisions show a progressive lateral transition to cleaner H1 or H1b sandstone (e.g. *Beds 9* and *16.1* in M. Ramaceto section), and (2) beds

with laterally continuous H3 divisions with well-defined, sharp contacts with underlying H1 divisions that are rugose (e.g. *Beds 9.3* and *18.3* in the M.Ramaceto section; *Beds a, b* and *c* at Ballybunion, the Mam Tor HEBs). Heterogeneity in both cases principally reflects variable development of the H3 division in what are otherwise sheet-like event beds; a secondary heterogeneity can be attributed to lateral changes in the expression of the overlying sandy H4 division and its interaction with H3, where present. The origin of both the principal and secondary styles of heterogeneity is now discussed, beginning with the variable development of the H3 division, which is more critical to reservoir properties in that it replaces clean and better quality sandstone laterally.

# 5.1. Variable proportions of H1 and H3 divisions

Four mechanisms may account for the observed lateral variability in H3 (Fig. 13). The first is applicable to those cases where the H3 division is discontinuous and transitions laterally into cleaner sandstones containing abundant mudstone clasts (Type 1 heterogeneity above); the others apply to cases where the H3 division is continuous and distinct from the underlying clean mudclast-poor or free H1 sandstone (Type 2).

Where the H3 division is discontinuous and forms lenses that merge laterally with cleaner sandstone, diffuse lateral boundaries appear to be preferentially developed immediately adjacent to where the H1 sandstone has a convex-up top; in these beds discrete transitions preferentially occur beneath downward-convex H1/H3 contact (Fig 13A). Such a geometry is particularly well-developed in the cases where there are short-scale (10s m) lateral changes between fully-developed hybrid event beds and turbidite beds with abundant mudstone clasts surrounded by relatively clean sandstone. The presence of mudstone clasts in both the H1 and H3 divisions (generally more abundant in the latter) suggests that the patchy H3 division may reflect deposition from a flow in which the process of transformation to create a linked debrite was either partial or incomplete (Patacci et al., 2014). Examples of this kind of lateral relationship are provided by *Beds 9* and *16.1* in the Ramaceto sections and by the B and C type lateral transitions in the Cilento case study (Fig. 12).

Postma et al. (1988) showed that low-density mudclasts entrained by a high-density turbidity current can be suspended by strong turbulent lift and buoyancy forces before eventually settling to collect at the boundary between a basal high-concentrated inertia-flow layer and an overlying, faster moving turbulent-flow layer. They may be transported there either rafted on top of the high-concentration layer and/or propelled by the

overlying turbulent part of the flow. Rapid suspension deposition from the denser portion of the turbidity current may then freeze the collection of mud clasts in-situ, burying them in clean sand (Mutti and Nilsen, 1981). Alternatively, given sufficient concentration of clasts and dispersed clay, and with progressive disaggregation of the mud clasts, the clast-enriched basal part of the flow may evolve to form a linked cohesive flow (Haughton et al., 2009). There may be a threshold of mud concentration originating from clast disintegration that needs to be exceeded before such a transformation is possible – with the threshold itself a function of the overall flow turbulent energy. Larger more energetic flows will be harder to damp than smaller flows or those already decelerating and shedding turbulence. The discontinuous H3 divisions with diffuse and steep lateral margins suggest that in these cases the deposit preserves patchy transformation. One explanation for this is that it reflects spatially-variable patterns of clast entrainment and hence bed erosion up-dip. Alternatively the clasts may have been hydraulically concentrated into streamwise streaks or patches guided by large-scale longitudinal vortices in the flow. The vortices could define areas of negative velocity gradients flanked on either side by regions of positive fluctuations (Marusic et al., 2010). Such large-scale motions, referred to in fluid mechanics as superstructures, have been recognised in high Reynolds number turbulent flows above the near wall-layer (the log-region of turbulent boundary layer) in experimental and natural cases (Hutchins and Marusic, 2007). The implication is that mudclasts could be more concentrated along certain zones of the flow, effecting local transformation only when sufficiently abundant. Ultimately beds of this type are likely give insight into the early onset of hybrid flow development.

Where the H3 division is more continuous and less transitional with the underlying H1 division (Type 2 heterogeneity), the irregular geometry of the H1/H3 contact could have been generated by erosion of the previously deposited basal sand by the clast-rich debris flow (Fig. 13B) as suggested by Talling (2013). Cohesive debris flows are often considered not to be erosive (Pickering et al., 1989) partly because they can hydroplane and this reduces the resistance due to drag on the floor (Iverson, 1997; Mohring et al., 1998; Mulder and Alexander, 2001). Nevertheless, field (Dakin et al., 2013) and seismic evidences (Moscardelli et al., 2006) suggest that such flows can erode and may even produce megascours in base-of-slope settings. Ploughing of the lower sand by larger blocks entrained in and propelled by the H3 debrite could excavate groove-like depressions in the H1 sand, and in places may completely remove it. The process implies entrainment of non-lithified just-deposited sand (i.e., the top part of H1) into the overriding debris flow

(Mohring et al., 1999), initially as sand patches. This model is applicable to the basal bed of the Ross example, to the Mam Tor *a*, *b*, *d*, *e Beds* and to b and c-transformations of the Cilento example. In particular, the linked-debrite of *Bed d* of the Mam Tor case study appears to have had an erosive character as it was able to scour into a previously deposited H2 banded interval (Fig. 8A). In many examples, the thickness of the material eroded matches that of the subsequently deposited by the linked debris flow to maintain the overall bed thickness. This implies erosion and emplacement of the linked debris flow were closely linked and that the debris flow is self-levelling and thus mechanically weak. It is also possible that shearing beneath the trailing flow that deposits H4 contributes to levelling of the H3 division.

A second option for the interpretation of continuous but thickness changing H3 divisions is that the debrite behaves as a coherent body that after deposition loads into the freshly deposited, water-saturated H1 sand (Fig. 13C). The dewatering processes can be promoted by the hydraulic pressure created during emplacement of H3 onto a saturated, porous and permeable sand with the former acting as an impermeable barrier (especially when charged with large mud blocks). The effects are evident in the structure of both H1 and H3 divisions, with the former commonly rich in deformed dewatering sheets and dish structures and the later cross-cut by upward-extruding sand dykes. As the flow transformation to generate the linked debris flow may be patchy up-dip, the debris flow may vary in density locally, reflecting the variable entrained mud concentration. The differential loading of the high porosity basal H1 sandstone causes it to deform and along with water expulsion leads to upward sand doming and sand-injections, modifying what may have been an originally planar H1/H3 contact. The loading and dewatering must happen before deposition of the H4 division, because no injections were observed to cross-cut the H3/H4 boundary (see later). Locally, foundered balls of muddy sandstone occur within the H1 division, the phenomenon being particularly well developed where the linked-debris flow is able to carry large substrate blocks as in Bed 9.3 of Gottero case study and in the basal Ross Formation in Ballybunion (Bed b – Fig. 9, in which the H3 debrite is able to load the unconsolidated basal sand reducing its thickness to just few centimetres). Similar processes have been interpreted in subsurface studies, e.g., inclined contacts at the base of H3 divisions in core, parallel to rotated shear fabrics in the overlying debrite, imply downward foundering of the debrite (Haughton et al. 2003). The loading mechanism may explain why some beds with H3 divisions pass down-dip into beds dominated by

clean sandstone; the debris flow can be decelerated to the point of arrest as it loads and founders into its sandy substrate. Loading and ploughing need not be mutually exclusive.

Another cause of rugosity along the H1/H3 contact is that it could have been generated by m-scale sandy bedforms at the top of H1 sandstone that were subsequently buried by a linked debris flow (Fig. 13D). This explanation might apply where linked debrites overlie a metre-scale, regularly undulated top to H1 (e.g. *Bed 18.3* in the M. Ramaceto succession). The undulations would resemble megaripple-like bedforms (F6-like *sensu* Mutti, 1992; Mutti et al., 2003) or hummocky-type bedforms (Pickering and Hiscott, 1985; Remacha et al. 2005; Muzzi Magalhaes and Tinterri, 2010; Tinterri, 2011). Three-dimensional dunes have been reported by Talling et al. (2007a; 2012; 2013) at the top of H1 divisions in Marnoso Arenacea Formation. However, the lack of H1 cross-lamination in all of the four case studies rules out this explanation in these cases. Furthermore, some of the H1/H3 boundaries in both the present work and in Hodgson (2009) are too steep to represent passive filling of underlying bedforms, although post depositional loading of H3 into H1 could cause later steepening.

# 5.2. Nature of the H3/H4 boundary

Hybrid event beds commonly have an upper H4 division of fine to very fine sand grading into silt. This division generally displays traction and traction-plus-fallout structures, commonly with ripples at the base (often convoluted), overlain by parallel wavy laminae and parallel planar laminae. This division is interpreted as the deposit of a low-density turbidity current wake, implying a return to non-cohesive behaviour after the deposition of the H3 linked-debrite (Haughton et al., 2009). H4 divisions are almost always present in the Gottero and Cilento case studies, but are absent in Mam Tor, where the debrite (H3) is generally directly overlain by mudstone (H5).

The H3/H4 boundary has a wide range of geometries in the studied examples (Fig. 14). It can be a planar sheet comprising parallel- or rippled-laminated sandstone. It can also show growth structures, preserved in the pattern of laminations at the base of the H4 division (Fig. 14B), which can be asymmetric, suggesting that the deposition occurred when the underlying H3 debrite was still moving and deforming (Butler and McCaffrey, 2010; Patacci et al., 2014). As noted by Haughton et al. (2010) and Talling (2013) the H4 sandstone can load deeply into the H3 debrite, producing a m-scale undulated surface at the top of H3 (Fig.

14C). Loading can continue to the point where the H4 sandstone founders partially or completely into the debrite (Fig. 14D), where it may be further deformed, if H3 movement is ongoing. The geometry of the H3/H4 bounding surface may relate to the interpreted rheology of the linked-debrite (H3). A planar boundary suggests a semi-rigid behaviour of the underlying debrite, at least in its topmost part. When loading structures are present, a more plastic behaviour is inferred. Muddier and more chaotic H3 divisions commonly have loaded and foundered H4 divisions, while sandier and more homogeneous debrites preferentially have planar top surfaces.

In a few cases, the muddy debrite has an irregular interval of structureless and deformed sand, usually medium or coarse-grained, that occurs just at the base of the laminated H4 division (e.g. *Bed 9* and *9.3*, M. Ramaceto – Fig. 6A). Although this sand is relatively clean, it is not considered as part of the H4 division but is interpreted to have been emplaced by sand-dykes sourced in H1 that penetrate all the way through the H3 division.

#### 6. REVISED DEPOSITIONAL MODEL FOR HYBRID-PRONE LOBES

The short length-scale lateral variability in bed make-up documented above can be incorporated into a revised model of hybrid event bed – prone lobes (Fig.15). Many of the beds documented in the examples discussed above appear to represent the depositional record of the progressive change from a proximal clean high-density turbidites, into beds with mud clasts surrounded by clean sandstone, to various types of hybrid event beds decreasing progressively in thickness and increasing in mud dispersed in the H3 division. Relatively proximal, thick, coarse-grained beds containing mudstone clast clusters in patches 10s m across (Fig. 15, Transect 1) represent an incipient stage in the flow transformation process. These beds are thought to have been deposited from flows that were still mainly frictional (turbulent with dense sandy near bed layers), and had yet to partition into sections with contrasting rheology. The mudstone clasts are concentrated in bodies sandwiched between the structureless H1 and structured H4 deposits, but because the mudstone clasts float in a clean sandstone, the sector containing them cannot be considered the deposit of a linked-debris flow (H3). Such bodies are, however, interpreted to represent a precursor step to linked debrite formation downcurrent. At this stage, the frontal part of the flow was still erosional, suspending in some cases large quantities of mud clasts that were then buried in a relatively proximal position before they could

undergo significant transport, due to rapid collapse of the sandy suspension. The patchy distribution of clasts may represent heterogeneous erosion and/or hydraulic separation of entrained clasts, although fractionation can be less effective in cases where the clasts were rapidly buried by high suspended sand fall-out rates.

Immediately down-dip from the zone of erosion (Fig. 15; Transect 2), repeated lateral transitions between mudstone clast-rich high-density turbidites and hybrid event beds occur over lateral distances of 100-150 m (e.g. Bed 9 and 16.1 of Gottero Sandstone example). Although seen in 2D section, the geometry is here inferred to relate to complex interfingering between the up-dip sandstone-dominated part of the bed and the down-dip muddier section where mud clast-rich clusters had coalesced and began to flow independently as a H3 debris flows. Where event beds with H3 divisions are observed to pass downcurrent into cleaner sandstones (e.g., Fig. 12A), these are thought to be either highly oblique sections through elongate fingers or places where the debritic component of the bed has extended and broken and foundered. The scale of the fingers is thought to have been ultimately controlled by the pattern and concentration of the mud clasts and clay entrained in the flow; longitudinal vortices of flow superstructures could play a role in clast segregation (Hutchins and Marusic, 2007). At this stage the linked-debris flow may not have achieved the textural characteristics of a fully cohesive debrite as the amount of dispersed clay would have been relatively limited in comparison with more distal settings on account of the large quantity of clay still trapped in coherent and yet to disintegrate mud clasts. The clast rich-lenses and patches can be partly modified by loading, distension and upward-doming of the H1 clean and clast-poor sand, with sand injections above the muddy division creating sills along the H3/H4 boundary.

When the sediment gravity flow is fully partitioned into a frontal high-density turbidity current and a following debris flow, the resulting hybrid event bed can show variable internal proportions of the basal H1 sandstone and the upper linked-debrite with an overall constant bed thickness (Fig. 15; Transect 3). As shown by the examples discussed above, the rugosity on top of the clean sandstone division can have wavelengths varying from a few metres (e.g. *Bed 18.3* of M.Ramaceto section) to tens of metres (e.g. basal Ross Formation in and Mam Tor examples). It is best developed in relatively thick and coarse-grained hybrid event beds containing abundant clasts, including large rafts many metres across (e.g. *Bed 9.3* Gottero example). This supports the idea that the rugosity is a product of a combination of loading and clast

ploughing by a self-levelling debris flow. The rugosity is less apparent in the thinner and finer-grained hybrid event beds interpreted to have been deposited more distally or by less energetic flows (Fig. 15 - Transect 4). This may arise because decelerating linked debris flows are less energetic, and evolve to become more cohesive, or because the thinner H1 sandstone was formed in whole or in part by settling of sand through a muddy suspension as suggested by the experimental work on decelerating transitional clay-rich suspensions by Sumner et al. (2008) and Baas et al. (2011).

Transitions between hybrid event beds and thin low-density turbidity current deposits over very short distances (less than 150 m) in the Cilento Lago section and in Gottero Sandstone (*Bed 18.3* from Fig. 5A) are consistent with rapid down-dip (and lateral) pinch-out of the debritic component of the bed. Similar relationships have previously been inferred elsewhere and especially in the foredeep of Marnoso Arenacea Formation (Apennines, Italy) by Amy and Talling (2006) and Muzzi Magalhaes and Tinterri (2010) and in the Windermere Supergroup deep-water turbidite system, Canada (Terlaky and Arnott, 2014).

#### 7. IMPLICATIONS FOR RESERVOIR PERFORMANCE

Hybrid event beds are often important components in deep-water systems that form hydrocarbon reservoirs. Their presence tends to have a negative effect on reservoir volume and quality, due to the clay-rich texture of the H3 divisions which act as baffles to flow (Amy et al., 2009), and are associated with higher water saturations. Successions in which hybrid event beds dominate tend to exhibit tabular bed stacking, with poor vertical connectivity between the cleaner H1 sandstones. Examples of reservoirs where hybrid event beds influence hydrocarbons recovery efficiency include the Miller-Kingfisher fan, the Magnus-Penguin and Forties fan in North Sea (Haughton et al., 2003; Davis et al., 2009) and the Diana field and the Wilcox Formation, in the Gulf of Mexico (Sullivan and Templet, 2002; Kane and Ponten, 2012). The work detailed here shows that additional concerns regarding correlatability and sweep efficiency may arise where H1/H3 contacts are rugose.

Rapid lateral facies variability increases well correlation uncertainty at bed level as even wells only a few hundred metres apart could have beds with very different bed characteristics in core, and/or wireline signatures. Accordingly, three guidelines for well correlation in hybrid-dominated lobes are proposed: i) hybrid event beds are generally tabular, but can have variable internal make-up, changing from beds comprising almost exclusively clean sandstone to beds comprising clean and argillaceous sandstone at kilometre scale on along-flow transects, with heterogeneity possible at much shorter (i.e., 10 m) scale along across-flow transects; thus bed thickness may be a better guide to correlation than internal bed lithofacies; ii) abundant mudstone clasts in an up-current location could correlate with fully developed hybrid event beds in a downcurrent location; iii) the zone of transition is unlikely to be fixed, potentially moving both up- and downstream, at the scale of successive beds, and also within the larger scale stratigraphy. Thus the degree of correlatability, and the type of correlations to expect, are themselves hard to predict.

The rugosity along the top of the H1 sandstone is also an important production issue, particularly where WAG (Water-Alternating-Gas) improved oil recovery is employed to more efficiently sweep bed tops. A rugose H1/H3 boundary can partially strand oil at production timescales in the irregularities along the upper surface of the H1 sandstone. Conceptually, such rugosity could have two end-member forms (Fig.16): i) linear ridges elongated in the palaeoflow direction or ii) a more irregular "egg box" pattern, made up of domes and concavities. Although it is difficult to constrain the 3D shape in what are generally 2D outcrops, linear features resembling erosional furrows on the base of the overlying debrite are associated with short wavelength rugosity along the H1/H3 contact in more distal settings; the irregular "egg box" shape may be associated with differential loading of the debrite and consequential sand extrusion and injection of the overlying sandstone which could be more effective in presence of large muddy rafts in more proximal locations. The effect of partial reservoir compartmentalisation will be more evident when such irregularities are particularly pronounced (e.g. Bed 9.3 of M.Ramaceto or Bed a and c of Ballybunion) and the H3 muddydebrite thickens laterally on a scale of few tens of metres, with the basal sandstone reduced to a few centimetres or even completely removed. If the rugosity has a strong anisotropy (e.g., with linear ridges parallel to the original palaeoflow), the predicted sweep efficiency may vary depending on the relationship between any structural dip of the reservoir and the palaeoflow direction; where they align, a higher sweep efficiency along the structurally elevated areas of H1/H3 contact might be expected, with correspondingly poorer recoveries expected as they diverge.

### 8. CONCLUSIONS

Rapid internal facies variations are demonstrated in hybrid event beds drawn from a range of different types of basin and depositional locations within the system. Variability is expressed by beds with variable development of mudclast clusters in proximal positions, lateral transitions between debrite and clean sand containing mud clasts or, generally downstream, by abrupt changes in the basal proportions of clean sandstone to overlying muddy linked debrite; these variations can develop both across- and down-dip with respect to the palaeoflow direction, and can occur over very short distances (metres to 10s of metres). In each case the event beds retain an overall tabular geometry. These observations can be incorporated into a revised model describing the transition from up-dip clean turbiditic sandstone to down- and across-dip, HEB-dominated fringes via a transformation zone. This zone has a complex lobate and locally patchy geometry, captured in strike sections by repeated alternations between mud-rich debrites and relatively cleaner sandstone with scattered mudclasts expressed at the metre to 10s of m scale. The irregularities are best expressed in proximal transects but are present, albeit more subdued, in distal and thinner beds. Processes of water escape from basal clear sandstones, and associated injection of sand into overlying linked debrites together with processes of syn-depositional loading of sands into the linked debrite facies add further facies heterogeneity within the transformation zone.

Development of complex intra-bed geometries is thought to be the direct consequence of rapid but non-uniform flow rheology evolution from turbulent through to a progressively more cohesive state. Transformation processes are thought to reflect erosion of muddy substrate and the transport and breakdown of the eroded materials; the spatial variability of the transformation likely reflects a combination of locally patchy erosion and lateral segregation of clasts within the flow.

The variable thickness and continuity of the basal clean sandstone and the rugosity of its contact with the overlying debrite may impact hydrocarbon reservoir performance. Significant variability in bed character at inter-well scale can be anticipated, complicating correlation. Additionally, both intra-bed facies variability and the rugosity of the vertical contacts between facies may impact on drainage and sweep efficiency during production.

# 9. ACKNOWLEDGMENTS

This research was founded by Turbidite Research Group sponsors: Anadarko, BG Group, BP, ConocoPhillips, Dana Petroleum, Maersk Oil, Nexen, OMV, Petronas, Statoil, Tullow Oil and Woodside. We thank Marco Patacci for reading and providing constructive comments on an earlier version of the manuscript, Chris Davis for sharing the data regarding the Mam Tor case study and Luca Baruffini for the help in first reconnaissance of the M.Ramaceto area. Also we would like to thank the Associate Editor Thomas Hadlari, Carlo Messina and an anonymous reviewer for their helpful comments, which have considerably improved the final manuscript.

#### REFERENCES

Abbate, E. and Sagri, M., 1970. The eugeosynclinal sequences. Sedimentary Geology 4(3), 251-340.

Aitkenhead, N., Barclay, W.J., Brandon, A., Chadwick, R.A., Chisholm, J.I, Cooper, A.H. and Johnson, E.W., 2002. British Regional Geology of the Pennines and adjacent areas (Forth Edition), British Geological Survey, Nottingham, 206 pp.

Allen, C.R., 1960. Geological criteria for evaluating seismicity. Geological Society of America Bulletin 86, 1041-1057.

Amy, L.A. and Talling, P.J., 2006. Anatomy of turbidites and linked debrites based on long distance ( $120 \times 30 \text{ km}$ ) bed correlation, Marnoso Arenacea Formation, Northern Apennines, Italy. Sedimentology 53, 161-212

Amy, L.A., Peatchy, S.A., Gardiner, A.A. and Talling, P.J., 2009. Prediction of hydrocarbon recovery from turbidite sandstones with linked-debrite facies: Numerical flow-simulation studies. Marine and Petroleum Geology 26, 2032-2043.

Baas, J.H and Best, J.L., 2002. Turbulence modulation in clay-rich sediment-laden flows and some implications for sediment deposition. Journal of Sedimentary Research 72, 3, 336-340.

Baas, J.H., Best, J.L. and Peakall, J., 2011. Depositional processes, bedform development and hybrid bed formation in rapidly decelerated cohesive (mud-sand) sediment flows. Sedimentology 58, 1953-1987. DOI: 10.1111/j.1365-3091.2011.01247.x

Baas, J.H., Best, J.L., Peakall, J. and Wang, M., 2009. A phase diagram for turbulent, transitional, and laminar clay suspension flows. Journal of Sedimentary Research 79, 162-183. DOI: 10.2110/jsr.2009.025

Barker, S., 2005. Spatial and temporal evolution of deep-marine particulate gravity currents: an experimental, subsurface and outcrop investigation. Ph.D thesis, University College Dublin

Barker, S.P, Haughton, P.D.W., McCaffrey, W.D., Archer, S.G. and Hakes, B., 2008. Development of rheological heterogeneity in clay-rich high-density turbidity currents: Aptian Britannia sandstone member, U.K. Continental shelf. Journal of Sedimentary Research 78, 45-68. DOI: 10.2110/jsr.2008.014

Bonardi, G., Amore, F.O., Ciampo, G., De Capoa, P., Miconnet, P. and Perrone, 1988. Il Complesso Liguride Auctt.: Stato delle conoscenze e problemi aperti sull'evoluzione pre-apenninica ed i suoi rapporti con l'arco calabro. Mem. Soc. Geol. It. 41, 17-35.

Bouma, H., 1962. Sedimentology of Some Flysch Deposits. Amsterdam, Elsevier, 168 pp.

Butler, R.W. and McCaffrey, W.D., 2010. Structural evolution and sediment entrainment in mass-transport complexes: outcrop studies from Italy. Journal of Geological Society London 167, 617-631. DOI: 10.1144/0016-76492009-041

Butler, R.W. and Tavarnelli, E., 2006. The structure and kinematics of substrate entrainment in high-concentration sandy turbidites: a field example from the Gorgoglione "flysh" of southern Italy. Sedimentology 53, 655-670.

Casnedi, R., 1982. Sedimentazione e tettonica della unità liguri nell'Appennino nord-occidentale (Valli Lavagna-Sturla Trebbia e Aveto). Atti Ist. Geol. Univ. Pavia 30, 42-66.

Cavuoto, G., Martelli, L., Nardi, G. and Valente, A., 2007. Turbidite depositional systems and architectures, Cilento, Italy. In: Nilsen, T.H., Shew, R.D., Steffens G.S., and Studlick, eds. Atlas of deep-water outcrops: AAPG Studies in Geology 56, CD-ROM, 19 pp.

Cieszkovoski, M., Oszcypko, N., Pescatore, T., Slazka, A., Senatore, M.R., and Valente, A., 1995. Megatorbiditi Calcareo-Marnose nelle successioni slyscioidi dell'Appennino Meridionale (Cilento, Italia) e dei Carpazi Settentrionali (Polonia). Boll. Soc. Geol. It. 114, 67-88.

Collinson, J. D., 1988. Controls on Namurian sedimentation in the Central Province basins of northern England. Sedimentation in a synorogenic basin complex: the Upper Carboniferous of Northwest Europe. Blackie, Glasgow, 85, 101.

Dakin, N., Pickering, K.T., Mohring, D. and Bayliss, N.J., 2013. Marine and Petroleum Geology 41, 62-71. DOI:10.1016/j.marpetgeo.2012.07.007

Davis, C.E, 2012. Investigation into the origin and significance of hybrid event beds in mixed sand/mud deep sea fan systems. Ph.D thesis, University College Dublin.

Davis, C.E., Haughton, P.D.W., McCaffrey, W.D., Scott, E., Hogg, N. and Kitching, D., 2009. Marine and Petroleum Geology 26, 1919-1939. DOI: 10.1016/j.marpetgeo.2009.02.015

Eggenhuisen J.T., McCaffrey, W.D., Haughton, P.D.W., Butler, R.W.H., Moore, I., Jarvie and Hakes, W.G., 2010. Reconstructing large-scale remobilisation of deep-water deposits and its impact on sand-body architecture from cored wells: The Lower Cretaceous Britannia Sandstone Formation, UK North Sea. Marine and Petroleum Geology 27, 1595-1615. DOI:10.1016/j.marpetgeo.2010.04.005

Elliott, T., 2000. Depositional architecture of a sand-rich, channelized turbidite system: The Upper Carboniferous Ross Sandstone Formation, Western Ireland. Deep Reservoir of the World (2000), 342-373

Fugelli, E.M. and Olsen T.R., 2007. Delineating confined slope turbidite systems offshore mid-Norway: The Cretaceous deep-marine Lysing Formation. AAPG Bulletin 91, n. 11, 1577-1601.

Georgiopoulou, A., Wynn, R.B, Masson, D.G. and Frenz, M., 2009.Marine and Petroleum Geology 26, 2021-2031. DOI: 10.1016/j.marpetgeo.2009.02.010

Ghibaudo, G., 1992. Subaqueous sediment gravity flow deposits – practical criteria for their field description and classification. Sedimentology 39, 423-454

Haughton, P.D.W., Barker, S.P. and McCaffrey, W.D., 2003. "Linked" debrites in sand-rich turbidite systems – origin and significance. Sedimentology 50, 459-482

Haughton, P.D.W., Davis, C.E. and McCaffrey, W.D., 2009. Hybrid sediment gravity flow deposits – Classification, origin and significance. Marine and Petroleum Geology 26, 1900-1918.DOI: 10.1016/j.marpetgeo.2009.02.012

Haughton, P.D.W., Davis, C.E. and McCaffrey, W.D., 2010. Reply to Comment by R.Higgs on "Hybrid sediment gravity flow deposits – classification, origin and significance". Marine and Petroleum Geology 27, 2066-2069.

Hodgson, D.M, 2009. Distribution and origin of hybrid beds in sand-rich submarine fans of the Tanqua depocentre, Karoo Basin, South Africa. Marine and Petroleum Geology 26, 1940-1956.

DOI: 10.1016/j.marpetgeo.2009.02.011

Hodson, F., 1954. The beds above the Carboniferous Limestone in North-West County Clare, Eire. Quarterly Journal of the Geological Society, London 109, 259-283.

Hutchins, N. and Marusic, I., 2007. Evidence of very long meandering features in the logarithmic region of turbulent boundary layers. J.Fluid. Mech. 579, 1-28.

Ito, M., 2008. Downfan transformation from turbidity currents to debris flows at channel-to-lobe transitional zone: the Lower Plestiocene Otadai Formation, Boso Peninsula, Japan. Journal of Sedimentary Research, 78, 668-682. DOI: 20.2110/jsr.2008.076

Iverson, R.M., 1997. Physic of debris flows. Rev. Geophys. 35, 245-296

Jackson, C.A.L., Adli Zakaria, A., Johnson, H.D., Tongkul, F. and Crevello, P.D., 2009. Sedimentology, stratigraphic occurrence and origin of linked debrites in the West Crocker Formation (Oligo-Miocene), Sabah, NW Borneo. Marine and Petroleum Geology 26, 1957-1973. DOI: 10.1016/j.marinegeo.2009.02.019

Kane, I.A. and Ponten, A.S.M., 2012. Subamarine transitional flow deposits in the Paleogene Gulf of Mexico. Geology 40, n. 12, 1119-1122. DOI: 10.1130/G33410.1

Kneller, B.C. and McCaffrey, W.D., 1999. Depositional effects of flow nonuniformity and stratification within turbidity currents approaching a bounding slope: deflection, reflection, and facies variation. Journal of Sedimentary Research 69, 5, 980-991.

Kneller, B.C. and McCaffrey, W.D., 2003. The interpretation of vertical sequences in turbidite beds: the influence of longitudinal flow structure. Journal of Sedimentary Research 73, 706-713.

Lee, S.O., Jung, W-Y, Bahk J.J., Gardner, J.M., Kim, J.K. and Lee S.H., 2013. Depositional features of cogenetic turbidite-debrite beds and possible mechanisms for their formation in distal lobated bodies beyond the base-of-slope, Ulleung Basin, East Sea (Japan Sea). Marine Geology 346, 124-140. DOI:10.1016/j.margeo.2013.09.001

Lien T., Walker, R.G. and Martinsen, O.J., 2003. Turbidites in the Upper Carboniferous Ross Formation, western Ireland: reconstruction of a channel and spillover system. Sedimentology 50, 113-148.

Lowe, D.R. and Guy, M., 2000. Slurry-flow deposits in the Britannia Formation (Lower Cretaceous), North Sea: a new perspective on the turbidity current and debris flow problem. Sedimentology 47, 31-70.

Marini, M., 1992. L'Unità del M.Gottero fra la Val Trebbia e Sestri Levante (Appennino Ligure): nuovi dati di analisi di bacino e ipotesi di evoluzione sedimentaria. Boll. Soc. Geol. It. 111, 3-23.

Marini, M., 1994. Le Arenarie del M.Gottero nella sezione del M.Ramaceto (Unità del M.Gottero, Appennino ligure). Boll. Soc. Geol. It. 113, 283-302.

Marroni, M., 1991. Deformation history of the Mt. Gottero Unit (internal ligurid units, Northern Apennines). Boll. Soc. Geol. It. 110, 727-736.

Marroni, M., Meneghini, F. and Pandolfi, L, 2004. From accretion to exhumation in a fossil accrectionary wedge: a case history from Gottero unit (Northern Apennines, Italy). Geodinamica Acta 17, 41-53.

Martinsen, O.J., Collison, J.D. and Holdsworth, B.K., 1995. Millstone Grit cyclicity revisited II: sequence stratigraphy and sedimentary responses to changes of relative sea level. In: A.G. Plint, eds. Sedimentary Facies Analysis, A Tribute to the Work and teaching of Harold G. Reading. International Association of Sedimentologists Special Publication 22, 305-327.

Martinsesn, O.J., Lien, T., and Walker, R., 2000. Upper Carboniferous Deep Water Sediments, Western Ireland: Analogues for Passive Margin Turbidite Plays. In: GCSSEPM Foundation 20<sup>th</sup> Annual Research Conference, Deep-Water Reservoirs of the World, 533-555.

Marusic, I., Mathis, R., Hutchins, N., 2010. Predictive Model for Wall-Bounded Turbulent Flow. Science 329, 193-196.

Mohrig, D., Elverhøi, A. and Parker, G., 1999. Experiments on the relative mobility of muddy subaqueous and suberial debris flows, and their capacity to remobilize antecedent deposits. Marine Geology 154, 117-129.

Mohrig, D., Whipple, K.X., Hondzo, M., Ellis, C. and Parker, G., 1998. Hydroplaning of subaqueous debris flows. Geol. Soc. Am. Bull. 110, 387-394.

Moscardelli, L., Wood, L. and Mann, P., 2006. Mass-transport complexes and associated processes in the offshore area of Trinidad and Venezuela. American Association of Petroleum Geologists Bulletin 90, 1059-1088.

Mostardini, F. and Merlini, S., 1986. Appennino Centro-Meridionale. Sezioni geologiche e proposta di modello strutturale. Mem. Soc. Geol. It. 24, 107-131.

Mulder, T. and Alexander, J., 2001. The physical character of subaqueous sedimentary density flows and their deposits. Sedimentology 48, 269-299.

Mutti, E. and Nilsen, T.H., 1981. Significance of intraformational rip-up clasts in deep-sea fan deposits. Int. Assoc. Sedimentol. 2nd Eur. Reg. Meet. Bologna, 117-119.

Mutti, E., 1992. Turbidite Sandstones, AGIP, 275 pp.

Mutti, E., and Normark, W. R., 1987. Comparing examples of modern and ancient turbidite systems: problems and concepts. In Marine clastic sedimentology, 1-38. Springer Netherlands.

Mutti, E., Nilsen, T.H., and Ricci Lucchi, F., 1978. Outer fan depositional lobes of the Laga Formation (Upper Miocene and Lower Pliocene), East-Central Italy. In: Sedimentation in Submarine Canyons, Fans, and Trenches (Eds.), D.L. Stanley and G.Kelling, 201-223. Dowen Hutchinson & Ross, Stroudsburg.

Mutti, E., Tinterri, R., Benevelli, G., di Biase, D. and Cavanna, G., 2003. Deltaic, mixed and turbidite sedimentation of ancient foreland basins. Marine and Petroleum Geology 20, 733-755. DOI: 10.1016/j.marpetgeo.2003.09.001

Muzzi Magalhaes, P and Tinterri.R., 2010. Stratigraphy and depositional setting of slurry and contained (reflected) beds in the Marnoso-arenacea Formation (Langhian-Serravallian) Northern Apennines, Italy. Sedimentology 57, 1685-1720. DOI: 10.1111/j.1365-3091.2010.01160.x

Nardi, G., Bravi, S., Cammarosano, A., Cavuoto, G., Danna, M., De Rienzo, F., Martelli, L., Sgrosso, A., and Toccaceli, R.M., 2003. Carta Geologica regionale in scala 1:25.000 – Foglio 503 Vallo della Lucania. Regione Campania – Università degli Studi di Napoli Federico II.

Nilsen, T.H. and Abbate, E., 1984. Submarine-Fan facies associations of the Upper Cretaceous and Paleocene Gottero Sandstone, Ligurian Apennines, Italy. Geo-Marine Letters 3, 193-197.

Nilsen, T.H., Shew, R.D., Steffens, G.S. and Studlick, J.R.J., 2007. Atlas of deep-water outcrops: AAPG Studies in Geology 56, 504 p. and CD-ROM.

Parea, G.C., 1964. La provenienza dei clastici dell'Arenaria del M.Gottero. Atti Mem. Accad. Naz. Sci. Lettere Arti, Modena 6, 6. 1-7.

Patacca, E. and Scandone, P., 1989. Post-tortonian mountain building in the Apennines. In: A.Boriani, M. Bonafede, G.B. Piccardo and G.B. Vai, eds. Advances in Earth Science Research, Atti Conv. Accademia dei Lincei 80, 157-176.

Patacci, M., Haughton, P.D.W. and McCaffrey, W.D., 2014. Rheological complexity in sediment graivity flows forced to decelerate against a confining slope, Braux, SE France. Journal of Sedimentary Research 84, 270-277. DOI: 10.2110/jsr.2014.26

Pescatore, T.S., 1966. Strutture sedimentarie nel Flysch del Cilento occidentale. Geologica Romana 5, 99-116.

Pickering, K.T. and Hiscott, R.N., 1985. Contained (reflected) turbidity currents from the Middle Ordovician Cloridorme Formation, Quebec, Canada: an alternative to the antidune hypothesis. Sedimentology 32, 373-394.

Pickering, K.T., Hiscott, R.N. and Hein, F.J., 1989. Deep Marine Environments: Clastic Sedimentation and Tectonics. Unwin Hyman, London, 416 pp.

Postma, G., Nemec, W., Kleinspehn, K., 1988. Large floating clasts in turbidites: a mechanism for their emplacement. Sedimentary Geology 58, 47-61.

Pyles, D.R., Straub, K.M. and Stammer, G., 2013. Spatial variations in the composition of turbidites due to hydrodynamic fractionation. Geophysical Research Letters 40, 3919-3923. DOI: 10.1002/grl.50767

Pyles, D.R. and Jennette, D.C., 2009. Geometry and architectural associations of co-genetic debrite-turbidite beds in basin-margin strata, Carboniferous Ross Formation (Ireland): Applications to reservoirs located on the margins of structurally confined submarine fans. Marine and Petroleum Geology 26, 1974-1996.

Pyles, D.R., 2008. Multiscale stratigraphic analysis of a structurally confined submarine fan: Carboniferous Ross Sandstone, Ireland. A.A.P.G. Bulletin 92 (5), 557-587. DOI: 10.1306/01110807042

Remacha, E., Fernández, L.P. and Maestro, E, 2005. The transition between sheet-like lobe and basin plaon turbidites in the Hecho basin (south-central Pyrenees, Spain). Journal of Sedimentary Research 75, 789-819

Ricci Lucchi, F. and Valmori, E, 1980. Basin-wide turbidites in a Miocene, over-supplied deep-sea plain: a geometrical analysis. Sedimentology 27, 241-270.

Sylvester, Z. and Lowe, D.R., 2004. Textural trends in turbidites and slurry beds from the Oligocene flysch of the East Carpathians, Romania. Sedimentology 51, 945-972. DOI: 10.1111/j.1365-3091.2004.00653.x

Sullivan, M. and Templet, P., 2002. Characterisation of fine-grained deep-water turbidite reservoirs: examples from Diana sub-basin, Western Gulf of Mexico. Abstract presentation from GCSSEPM Deep-Water Core Workshop, Northern Gulf of Mexico, Houston, Texas, March 10, 2002.

Sumner, E., Amy, L., and Talling, P.J., 2008. Deposit structure and processes of sand deposition from a decelerating sediment suspension: Journal of Sedimentary Research 78, 529-547. DOI: 10.2110/jsr.2008.062

Talling, P. J., Malgesini, G., and Felletti, F., 2013. Can liquefied debris flows deposit clean sand over large areas of sea floor? Field evidence from the Marnoso-arenacea Formation, Italian Apennines. Sedimentology 60, 720-762. DOI: 10.1111/j.1365-3091.2012.01358.x

Talling, P.J. 2013. Hybrid submarine flows comprising turbidity current and cohesive debris flow: Deposits, theoretical and experimental analyses, and generalized models. Geosphere 9, 1-28. DOI:10.1130/GES00734.1

Talling, P.J., Amy, L.A., Wynn, R.B., Blackbourn, G. and Gibson, O., 2007a. Evolution of turbidity currents deduced from extensive thin turbidites: Marnoso Arenacea Formation (Miocene), Italian Apennines, Journal of Sedimentary Research 77, 172-196. DOI: 10.2110/jsr.2007.018

Talling, P.J., Amy, L.A., Wynn, R.B., Peakall and Robinson, M., 2004. Beds comprising debrite sandwiched within co-genetic turbidite: origin and widespread occurrence in distal depositional environments. Sedimentology 51, 163-194. DOI: 10.1046/j.1365-3091.2003.00617.x

Talling, P.J., Malgesini, G., Sumner, E.J., Amy, L.A., Felletti, F., Blackbourn, G., Nutt, C., Wilcox, C., Harding, I.C. and Akbari, S., 2012. Planform geometry, stacking pattern, and extrabasinal origin of low strength and intermediate strength cohesive debris flow deposits in the Marnoso-arenacea Formation, Italy. Geosphere, GES00734-1

Talling, P.J., Wynn, R.B., Masson, D.G., Frenz, M., Schiebel, R., Akhmetzhanov, A., Dallmeier-Tiessen, S., Benetti, S., Weaver, P.P.E., Georgiopoulou, A., Hotz, C., Cronin, B.T. and Amy, L.A., 2007b. Debris flow deposition from giant submarine flow begins far away from original landslide, Nature, 450, 541–544.

Terlaky, V. and Arnott, R.W.C., 2014. Matrix-rich and associated matrix-poor sandstones: Avulsion splays in slope and basin-floor strata. Sedimentology 61. 1175-1197. DOI: 10.1111/sed.12096

Tinterri, R., 2011. Combined flow sedimentary structures and the genetic link between sigmoidal- and hummocky-cross stratification. GeoActa 10, 1-43.

Tinterri, R., and Muzzi Magalhaes, P., 2011. Synsedimentary structural control on foredeep turbidites: An example from Miocene Marnoso-arenacea Formation, Northern Apennines, Italy. Marine and Petroleum Geology 28, 629-657. DOI: 10.1016/j.marpetgeo.2010.07.007

Valente, A., Ślączka, A. and Cavuoto, G., 2014. Soft-sediment deformation structures in seismically affected deep-sea Miocene turbidites (Cilento Basin, southern Italy). Geologos 20, 2, 67-78.

Van Vliet, A., 1978. Early Tertiary deepwater fans of Guipuzcoa, Northern Spain. In: Sedimentation in Submarine Canyons, Fans, and Trenches (Eds.), D.L. Stanley and G.Kelling, 190-209. Dowen Hutchinson & Ross, Stroudsburg.

Van de Kamp, P.C. and Leake, B.E., 1995. Petrology and geochemistry of siliciclastic rocks of mixed feldspatic and ophiolitic provenance in Northern Apennines, Italy. Chemical Geology 122, 1-20.

Walker, R.G., 1966. Shale Grit and Grindslow Shales: transition from turbidite to shallow water sediments in the Upper Carboniferous of Northern England. Journal of Sedimentary Petrology 36, 90-114.

Wood, A. and Smith, A.J., 1959. The sedimentation and sedimentary history of the Aberystwyth Grits (Upper Llandoverian). Quaterterly Journal of the Geological Society, London 114, 163-195.

Wynn, R.B., Kenyon, N.H., Masson, D.G., Stow, D.A.V., and Weaver, P.E., 2002. Characterisation and recognition of deep-water channel-lobe transitions zones. AAPG Bulletin 86, n. 8, 1441-1462.

Zeng, J.J., Lowe, D.R., Prior, D.B., Weiseman, W.J. and Bornhold, B.D., 1991. Flow proprieties of turbidity currents in Bute Inlet, British Columbia. Sedimentology 38, 975-996.DOI: 10.1111/j.1365-3091.1991.tb00367.x

## **CAPTIONS**

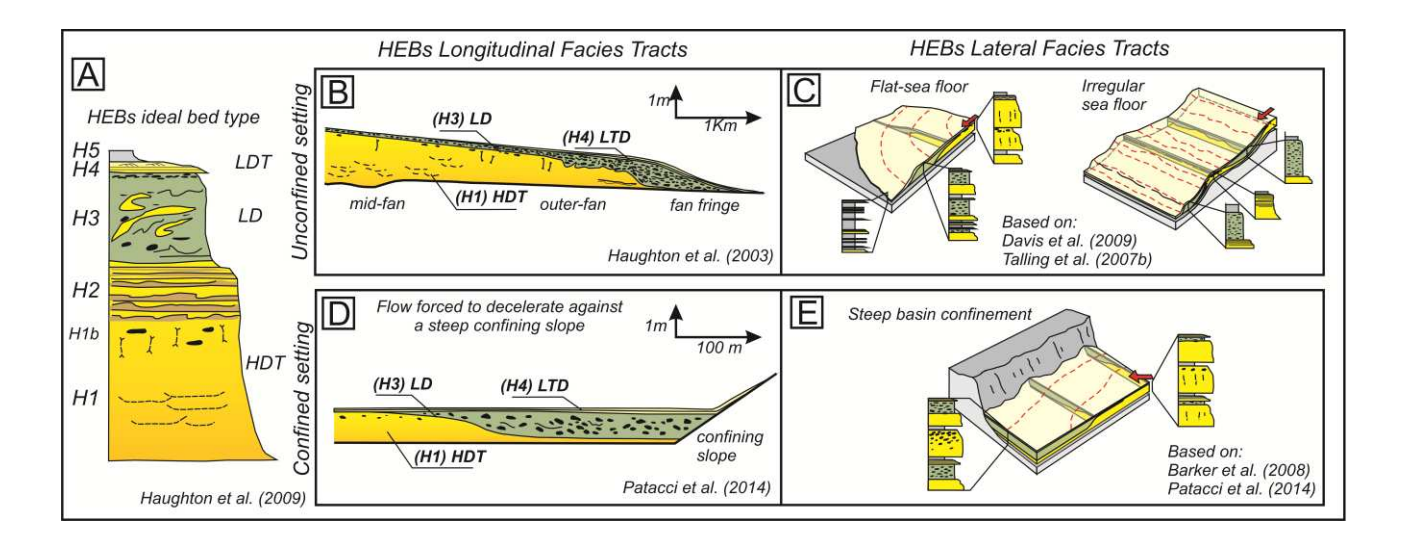


Figure 1 – Hybrid event bed type model and hybrid gravity flow facies tract expression. (A) Idealised organisation of a typical hybrid event bed (H1-H5 sequence) as suggested by Haughton et al. (2009). (B) Longitudinal facies tract expression of an hybrid flow deposit in unconfined setting: the mudclast-rich debritic H3 division progressively thickens down-dip in the outer fan and fan fringe fan sectors before finally pinching out (Haughton et al., 2003); facies transitions occur over several kilometres; (C) hybrid event beds are preferentially distributed in the marginal sectors of unconfined lobes (Davis et al., 2009) and influenced by local changes of gradient which make flatter areas prone to debris flow development and deposition (Talling et al., 2007b). (D) In obliquely confined settings the slope forces the flow to decelerate, rapidly damping turbulence and producing a transformation to cohesive flow which deposits close to the margin. (E) In laterally confined settings, thinner, slope-adjacent flows become less turbulent, becoming hybrid, and depositing hybrid event beds adjacent to the margin (HDT: high-density turbidite; LD: linked-debrite; LTD: low-density turbidite).

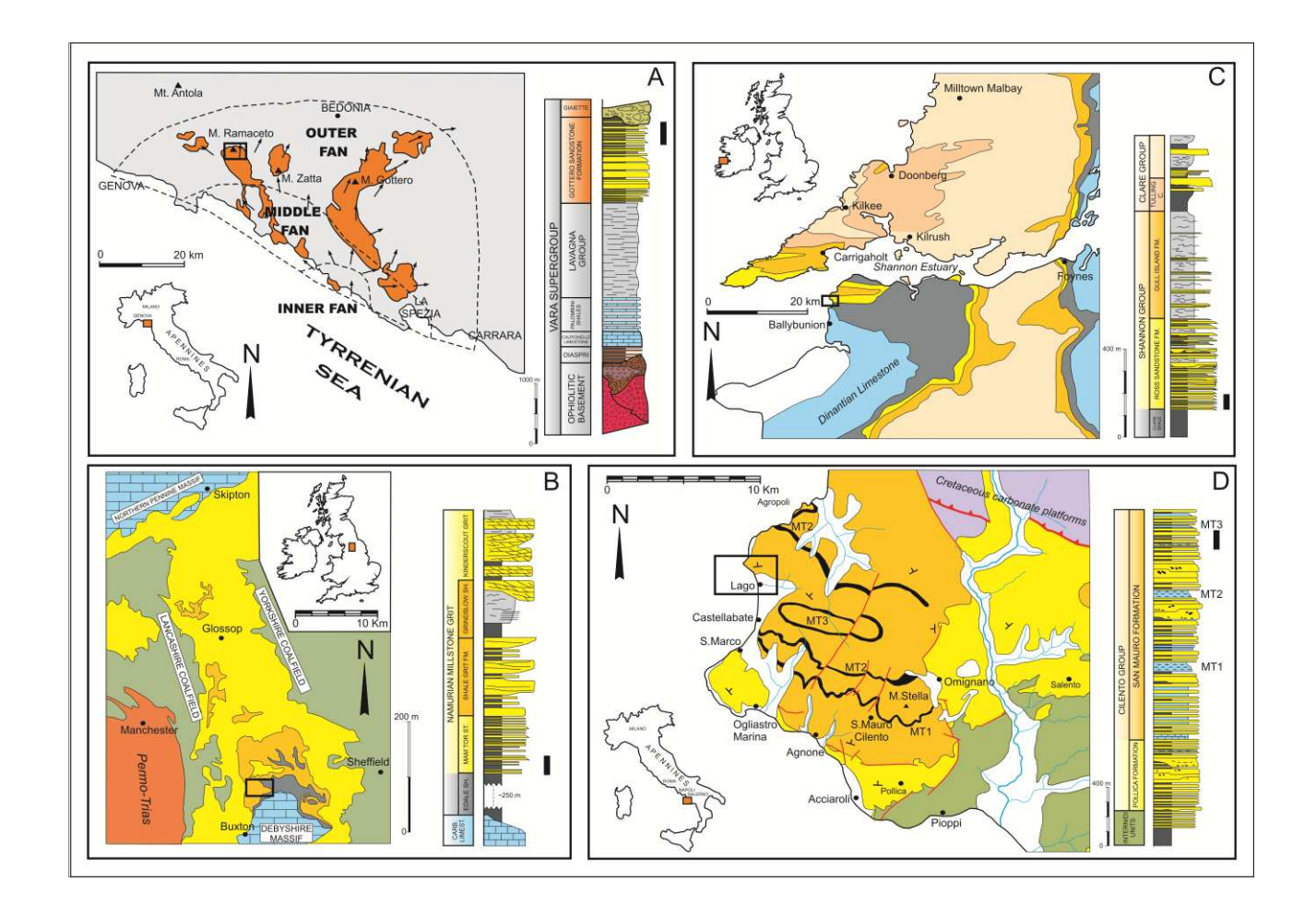
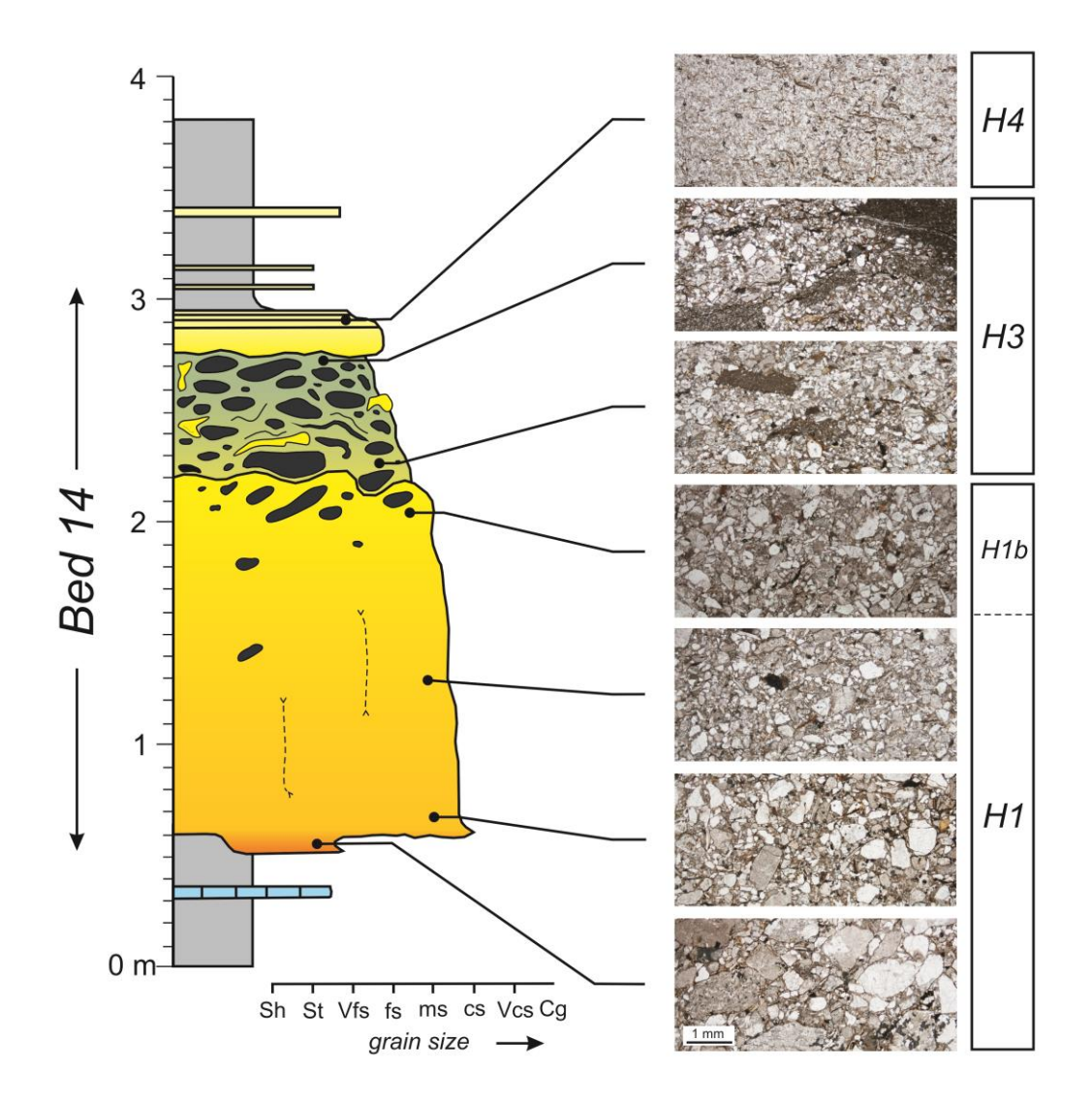
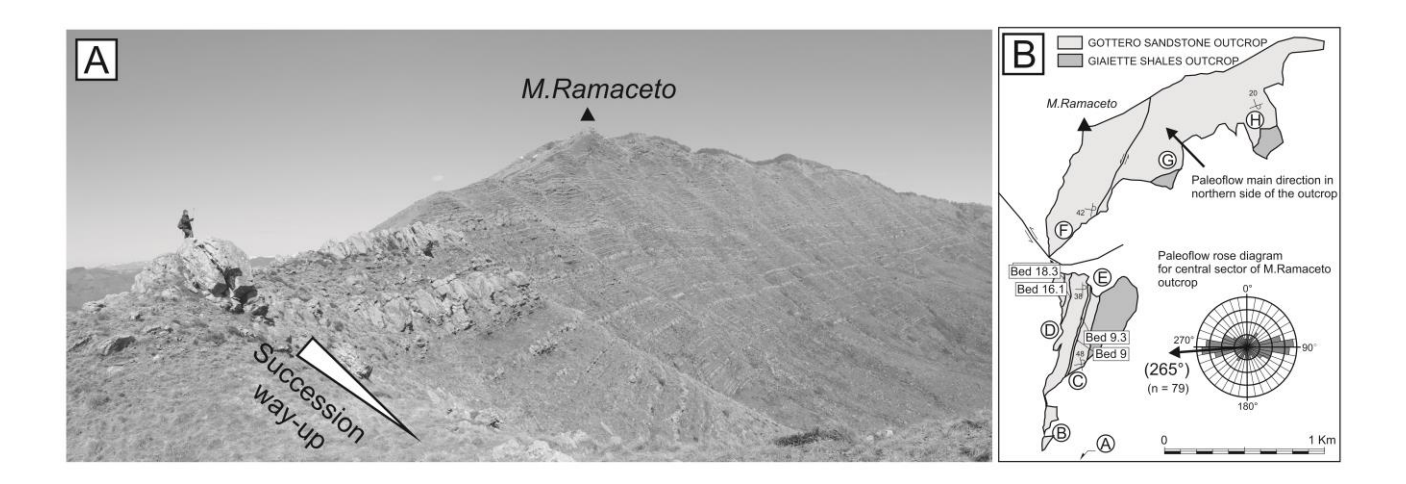


Figure 2 – Geological maps and regional stratigraphy of the four case studies. The colours on the maps correspond to those displayed in the stratigraphic logs; additional units are labelled. (A) Gottero Sandstone outcrop area in the north-western Apennines between Genova and Carrara (Italy) and stratigraphy of the Vara Supergroup comprising the Ligurian ophiolitic sequence (after Abbate and Sagri, 1970). The regional palaeoflow, the interpreted fan area and the distribution of the main facies associations are indicated (based on Nilsen and Abbate, 1984). (B) Mam Tor Sandstone outcrop location and the stratigraphy of Namurian basin in north England (after Walker, 1966). (C) Ross Formation outcrop in Co.Clare and Co. Kenny in western Ireland and stratigraphy of Shannon and Clare Group (based on Martinsen et al., 2000; Pyles, 2008). (D) Cilento Group in southern Italy with internal stratigraphic subdivisions (Nardi et al., 2003; Cavuoto et al., 2007). The black segments besides the stratigraphic column represent the stratigraphic intervals taken into account in this work and the squares on the map are the location of the field areas.



**Figure 3** – Bed profile and parallel light thin-section photographs of sandstone textures of a typical tripartite event bed from the Gottero Mount Ramaceto succession. The bed is characterised by distinct divisions: a graded relatively clean basal sandstone (very coarse to medium sand) with 10% average of dispersed clay (H1), with scattered mudclasts becoming more abundant towards the top (H1b); a chaotic mudclast-rich (up to 25 cm in size) muddy sandstone with a dispersed clay ratio about 20% increasing towards the top (H3); and a parallel and planar laminated fine-grained cap (H4).



**Figure 4** – Exposure conditions of the Gottero Sandstone in Mount Ramaceto area; note that the succession is inverted. (A) Landscape view of the outcrop highlighting its lateral extent and bed continuity. The photo captures about half of the 4 km wide exposure. (B) Map representing the outcrop areas, the locations of the measured logs shown in Fig. 5 and 6 and the orientation of the beds considered in this study with respect to the palaeoflow. The rose diagram shows the main palaeoflow orientation in the central sector of Ramaceto outcrop (sections C, D, E). The Giaiette Shales comprise a chaotic unit (MTC) overlying the Gottero sandstone.

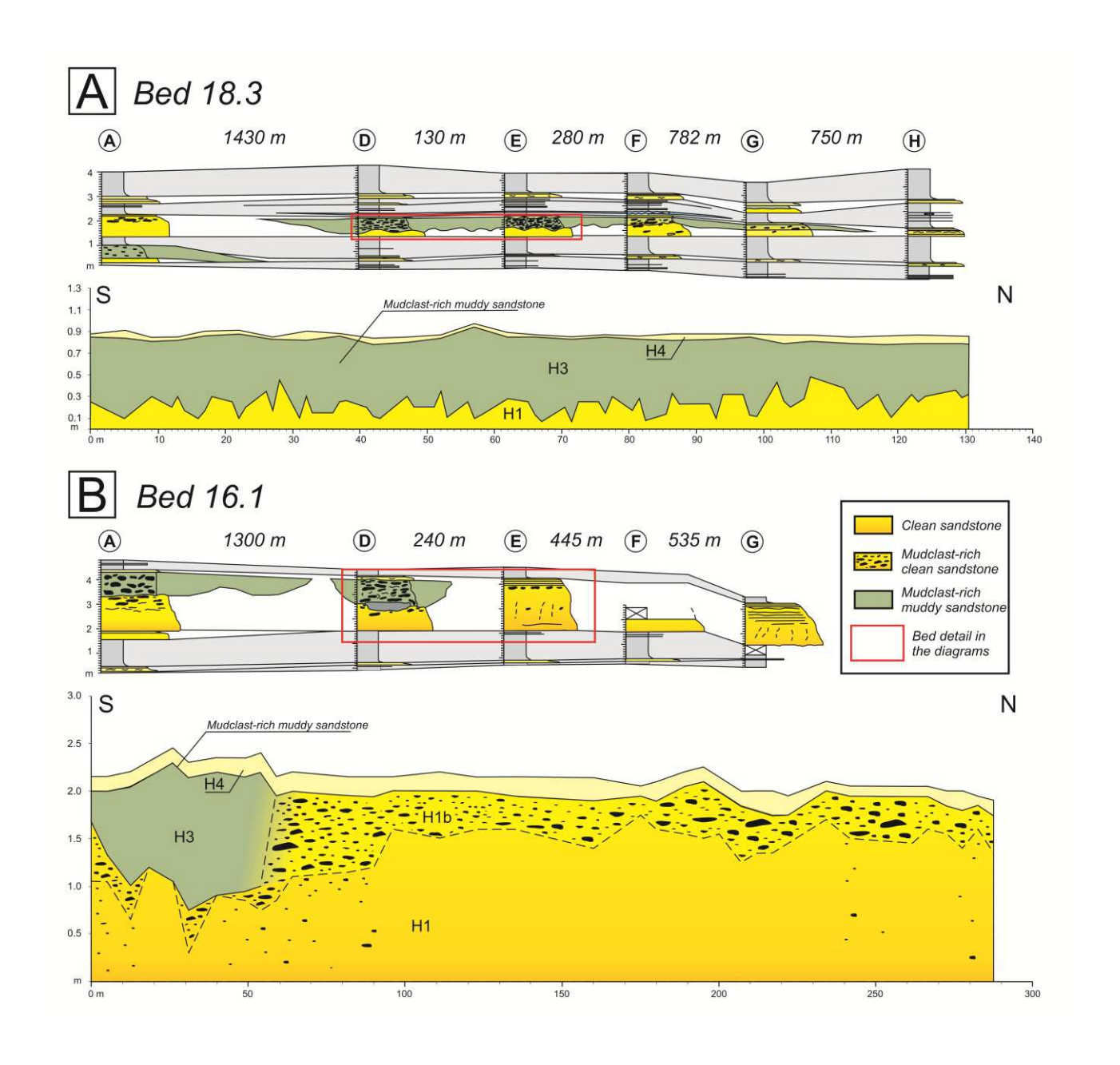


**Figure 5** - Lateral facies variability in *Beds 18.3* and *16.1* of the M. Ramaceto succession. The red squares indicate the areas represented in the underlying graphs which show the variable proportion and thickness change in the bed divisions: (A) *Bed 18.3* has m-scale irregularities along the H1/H3 contact. (B) *Bed 16.1* delineates the scale of lateral transitions between mudclast-rich but relatively clean sandstone bed and hybrid event bed.

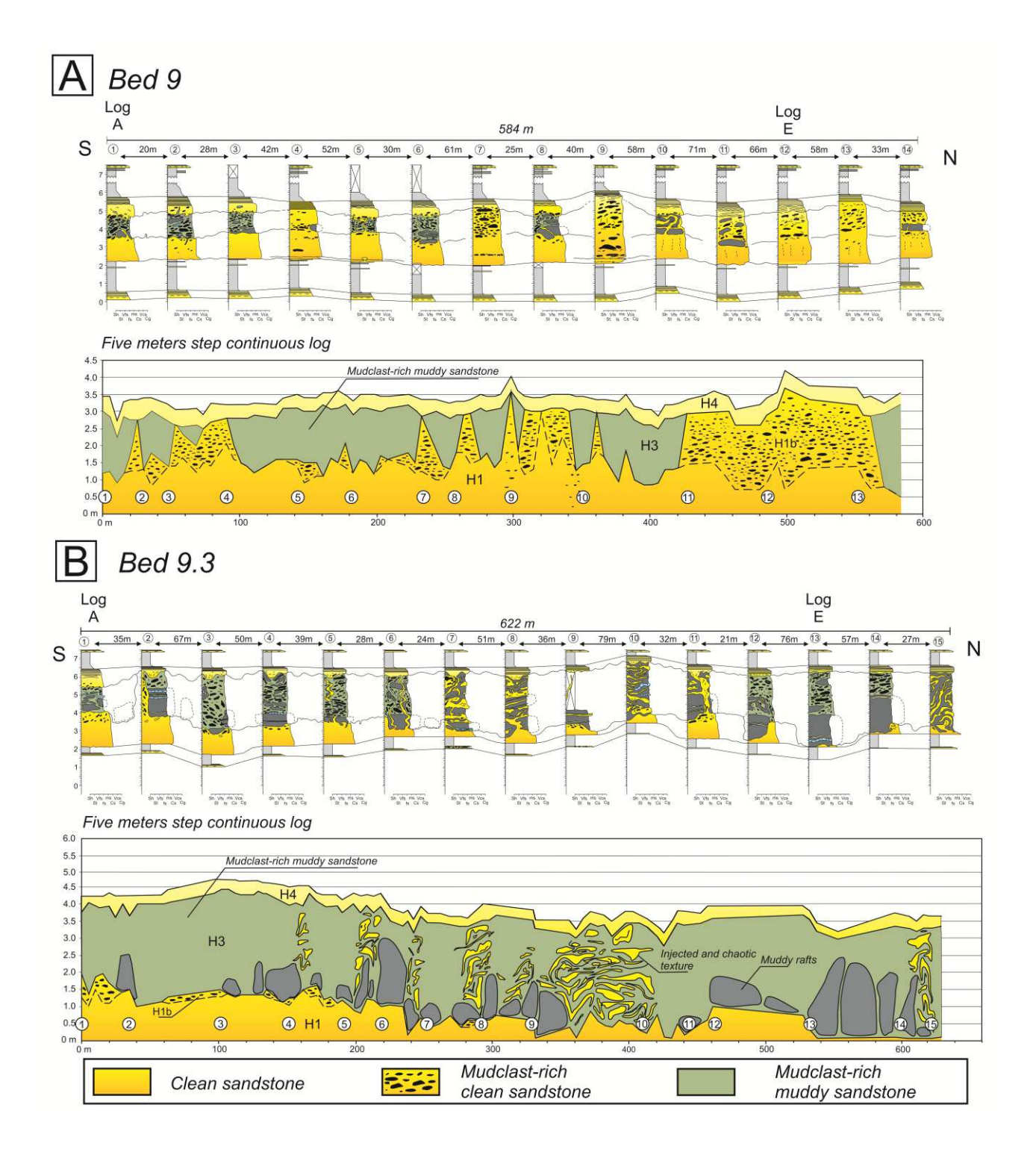


**Figure 6** - Lateral facies variability, bed profiles and internal thickness changes within *Beds 9* and *9.3* of the M.Ramaceto succession: (A) *Bed 9*, capturing rapid lateral transitions between mudclast-rich clean sandstone and mudclast-rich muddy sandstone on the 100-150 m scale; (B) *Bed 9.3* is a 4.5 m thick muddy HEB characterised in its H3 division by large muddy rafts surrounded by upward sand-injections mixed in a mudclast-rich dirty sandstone. The basal sand tends to taper towards north compensated by the corresponding increase of thickness of the H3 division, where the largest muddy rafts are found. In both beds

the H3/H4 boundary is more regular at 5 m scale in comparison to *Bed 18.3* of Figure 5A, but does show m-scale loading features of the H4 laminated sandstone into the underlying H3 muddier division.

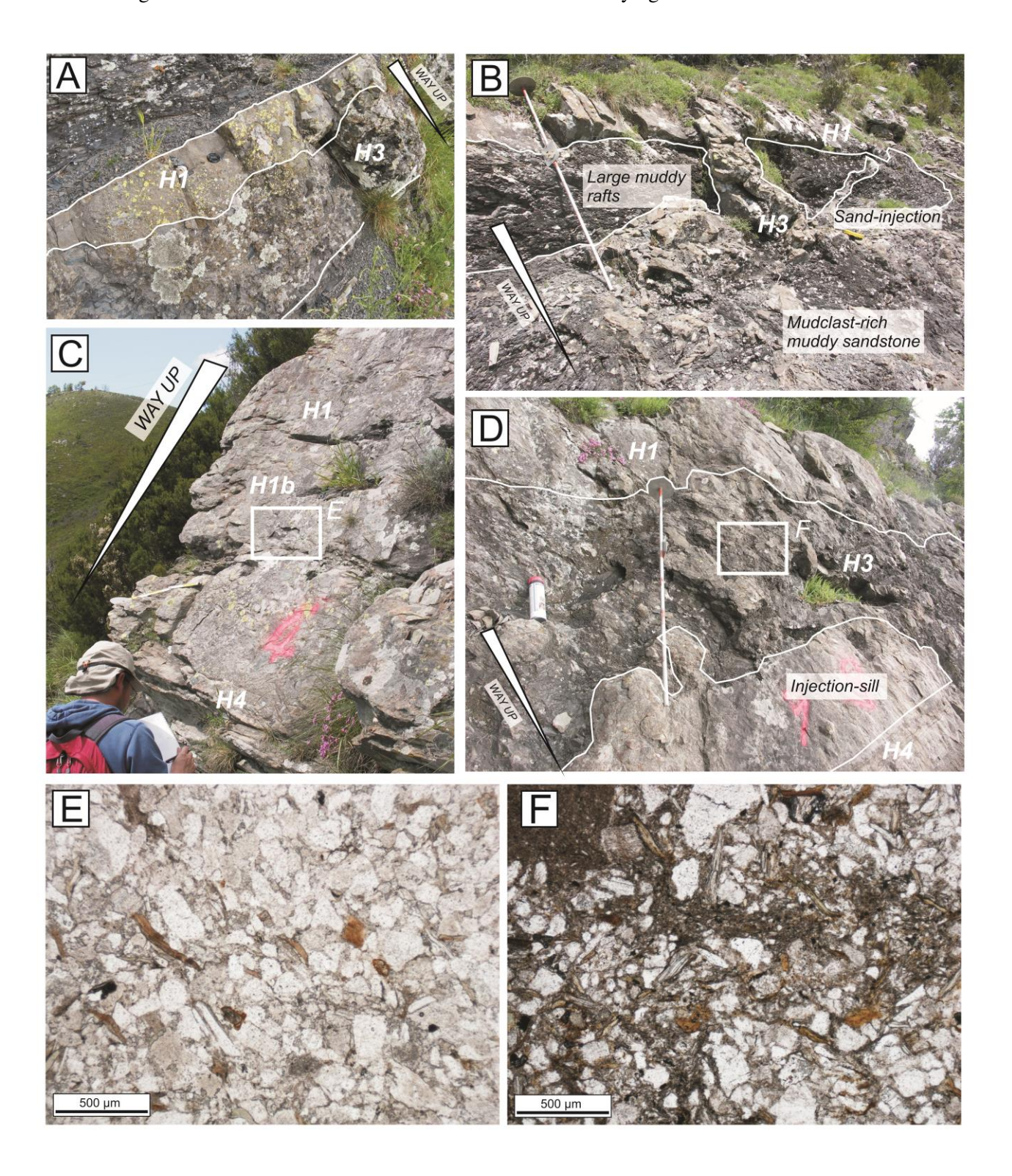


**Figure 7** – Bed types and textures from the M.Ramaceto section (way-up indicated): (A) *Bed 18.3* showing m-scale thickness changes between a cleaner H1 sandstone base and the H3 mudclast-rich muddy sandstone – 5 cm diameter camera lens cap as scale; (B) *Bed 9.3* (location 2 on Fig. 6B) characterised by large muddy

rafts, surrounded by large columnar and diagonal sand-injections, overlain by a mudclast-rich debrite; 1.5 m long Jacob staff as scale; (C) and (D) are different lateral expression of the central division (i.e., H3 or H1b) of *Bed 9* (see Fig.1 for definitions), and are less than 120 m apart (locations 4 and 8 on Fig. 6 respectively). (C) H1b scattered mudclasts surrounded by clean sandstone in the intermediate part of the bed; in (D) the same interval is expressed as an H3 mudclast-rich muddy sandstone, and is overlain by a clean sandstone injection sill developed at the H3/H4 boundary. The textures of these sandstones are shown in plane polarised light thin-sections in (E) and (F), in which there is a greater proportion of pore-filling clay present in F compared to E (20.4 against 12%), in addition to a higher proportion of mudclasts.

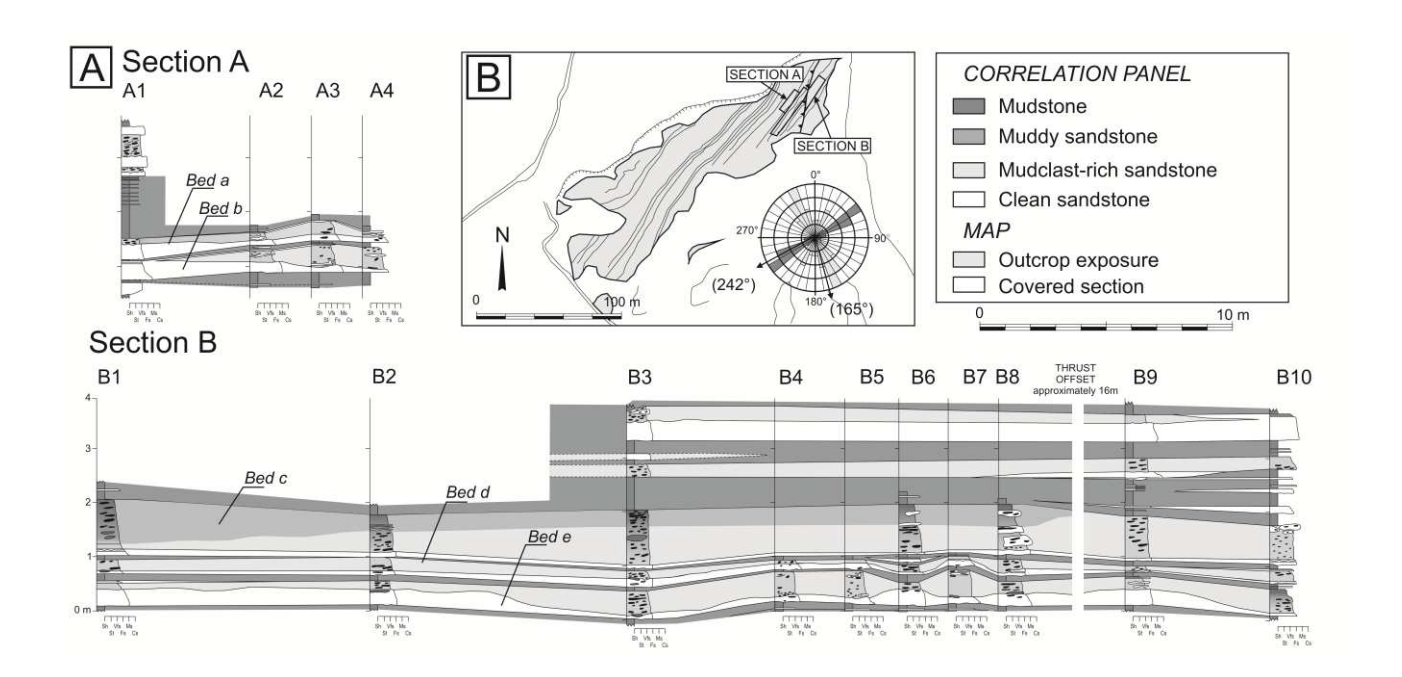


**Figure 8** – Map and correlation panel of the basal Mam Tor Sandstone in Mam Tor locality (northern England). (A) Detailed cross-sections highlighting the lateral variability of lithofacies; the combined lateral extent of the two sections is c. 70 m long after restoration of c.16 m displacement on an intervening thrust fault. (B) Schematic map of the outcrop with the orientation of main bedding planes and the palaeoflow orientation of the basal (dark grey) and upper part (light grey) parts of the succession indicated. Cross-section panels are modified from Davis (2012).

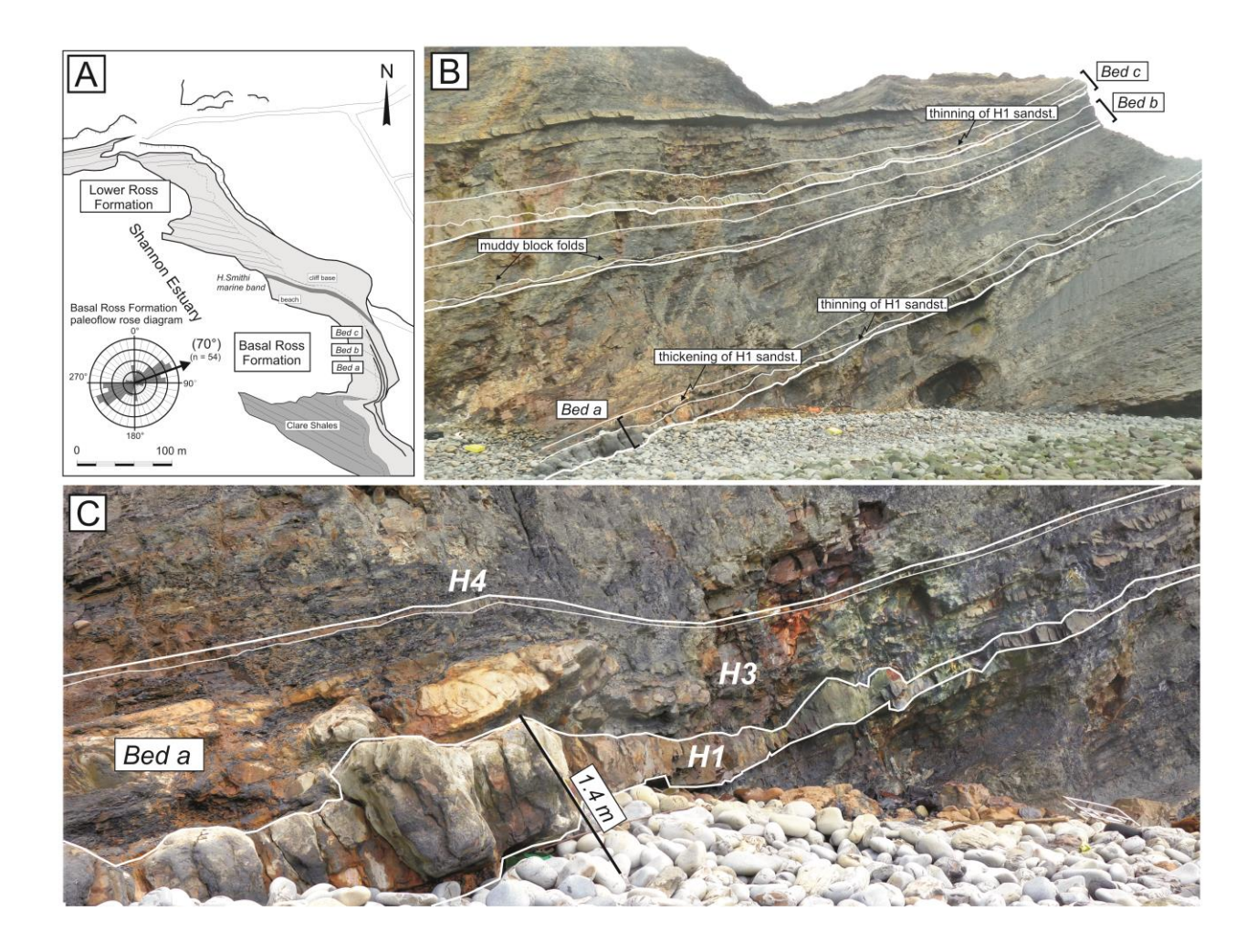


**Figure 9** – Map and outcrop view of Ballybunion section (Ross Formation, Western Ireland): (A) Outcrop location and the orientation with respect to the main palaeoflow orientation. The basal Ross unit is about 32 m thick in the Ballybunion location. (B) Bed traces of three HEBs cropping out in the basal part of Ross Formation with changes in the relative proportions of H1 and H3 indicated; The succession represented is 14 m thick from the base of *Bed a to the* top of *Bed* c and the photo show a 30 m wide lateral exposure. (C) Detail of *Bed a* outcrop exposure characterised by a 0.1 – 1.0 m thick, H1 basal sandstone division, with abundant pipe dewatering features overlain by a 1.0 to 1.5 m thick H3 division, with basal sandy-raft and a mudclast-rich muddy sandstone top and a fine grained 0.1 m thick H4 division. The H1/H3 contact is sharp but highly undulatory, resulting in thickness variation of the order of 0.7 m in both divisions – 1.4 m long Jacob staff is highlighted for scale.

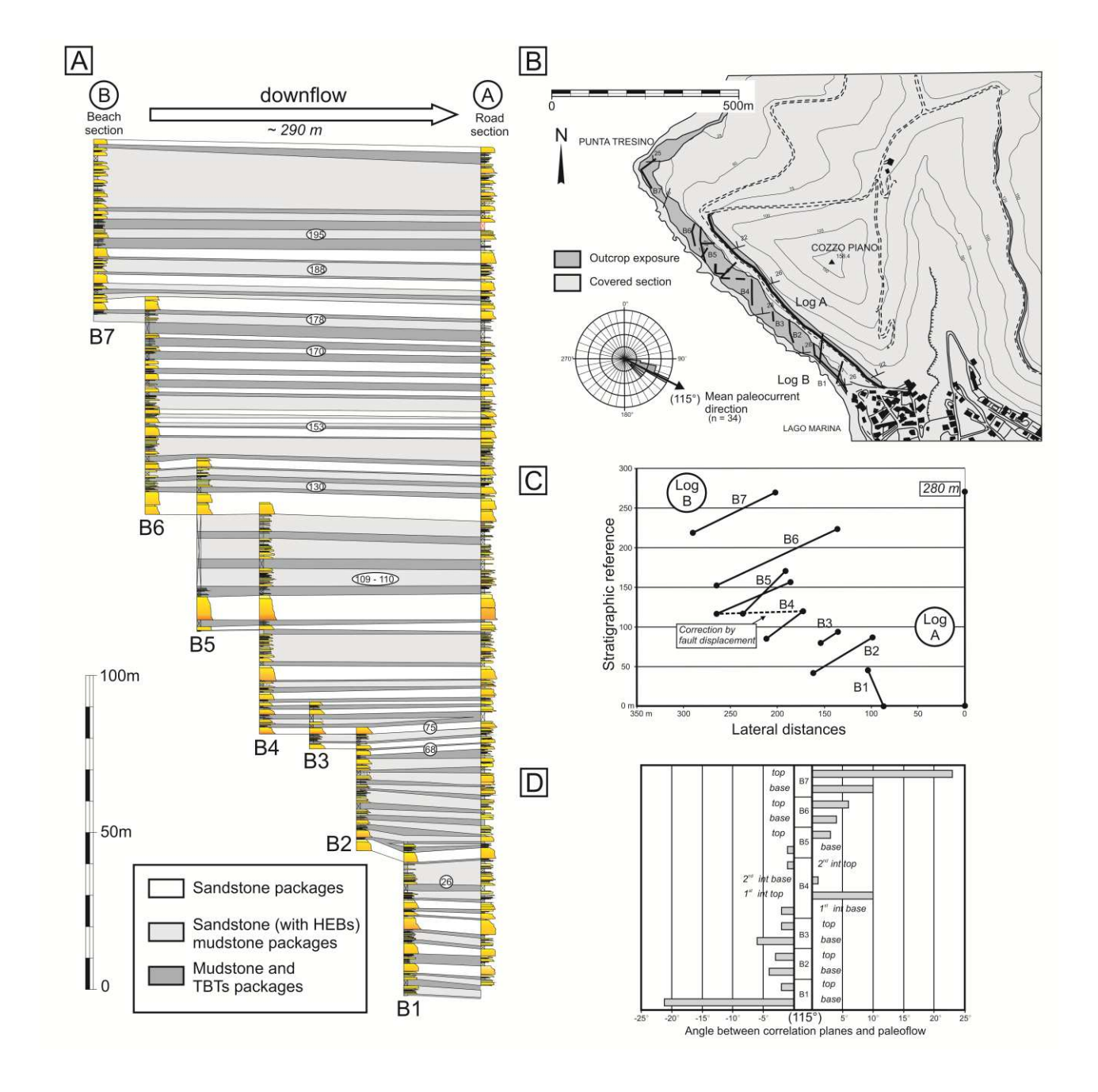


**Figure 10** – (A) Simplified correlation panel of the Lago succession of the Cilento Formation, in which the main facies associations and individual event beds have been traced, when possible, between the two main sections (the beach section is composed by seven logs measured along the beach cliff). The succession is punctuated by few outsized sandstone beds that are easily traceable between the road and the beach cliff section and are usable as correlation markers (in white). They are interbedded with thinner HEBs and turbidites (in grey) and shaly intervals with thin-bedded turbidites (in dark grey). The numbers across the panel refer to the detail bed correlations highlighted in Fig. 13. On the basis of palaeoflow orientation, beds on the beach section can be considered relatively more proximal than their correlatives on the road section.

The spacing between the two sections is approximate due to the oblique orientation but varies from c. 85 to 290 metres. (B) Schematic map of the Lago outcrop with the location of the measured sedimentary logs, the main faults and a palaeocurrent rose diagram. (C) Graph representing the distances in metres of the beds correlated between the relatively proximal beach sections and the more distal road section at different stratigraphic levels; the dashed line represents the effect of a fault displacement in Log B4. (D) Relative orientations of the correlation planes between the measured logs (from beach to road section) and the main palaeocurrent vector (115°) confirming that the correlations are effectively longitudinal to the palaeoflow with a maximum deviation of +/- 23° and an average very close to zero. Log B4 is split into two sections due to fault displacement.

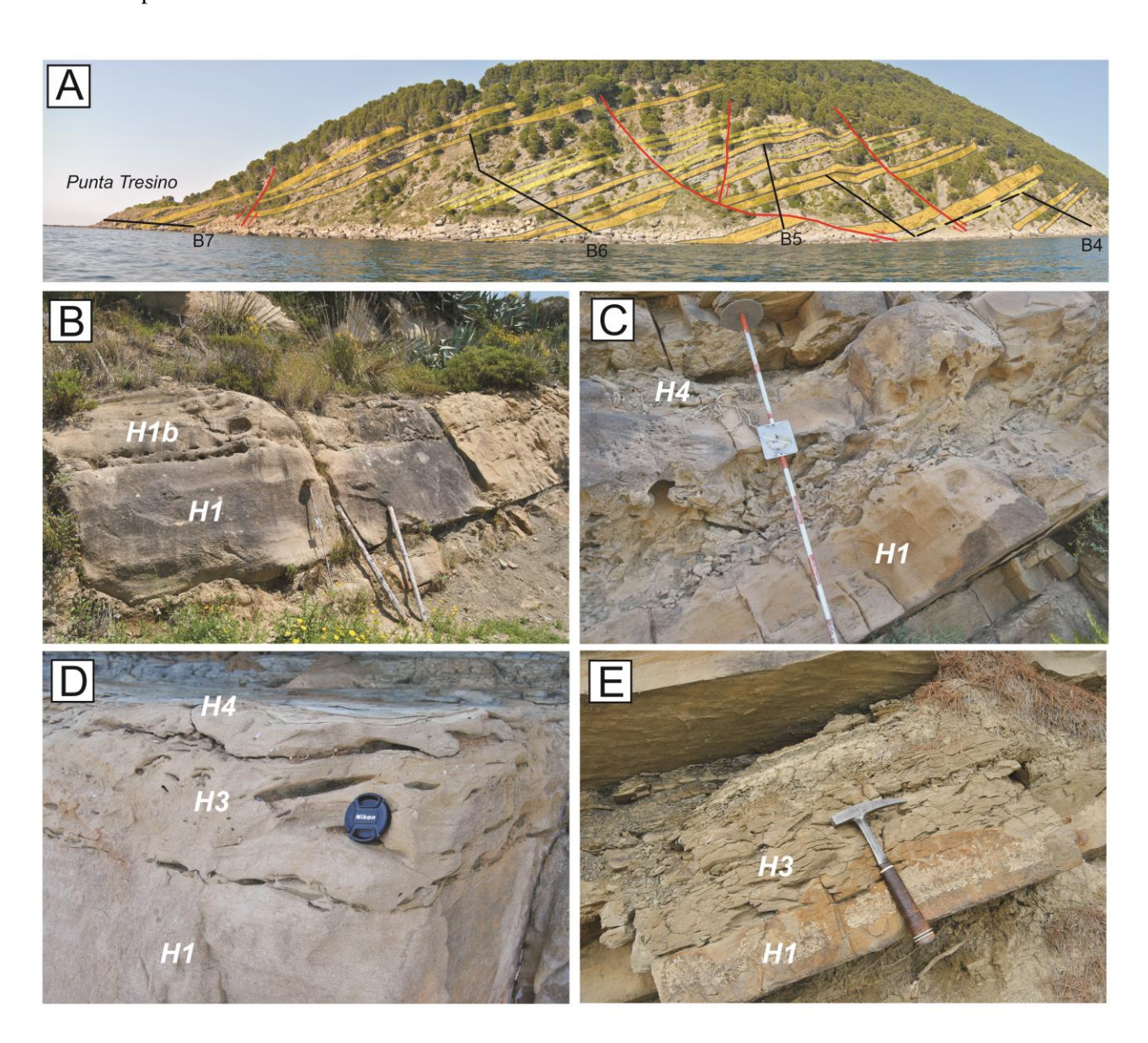


**Figure 11** – Representative photographs of bed types and outcrop exposure for the Lago section of the Cilento Formation. (A) The beach cliff overview of the Lago section shows the sheet-like geometry of the bed packages measured and correlated in the field (see correlation panel of Fig. 10A). The photo represents progressively younger sediments from south to north (right to left) in a 500 m wide view; small-displacement post-depositional faults do not affect the precise bed correlation. Colours are used to distinguish different bed packages to facilitate visualisation of the fault displacement. (B) 2.80 m thick sandstone bed with large mudclasts concentrated in the upper part of the bed, aligned along surfaces of crude lamination or concentrated in mudclast clusters (H1b division of Fig. 1) – 1.5 m long Jacob staff as scale. (C) 1.55 m thick bed with mudclast breccia in its central portion enclosed in clean sandstone. (D) A 0.35 m thick hybrid event bed made of a basal H1 clean dewatered sandstone, overlain by a slightly darker mudclast-rich H3 muddy sandstone, and capped by a thin ripple laminated sandstone – camera lens cap for scale. (E) 0.55 m thick hybrid event bed comprising a clean medium grained basal sand and a muddier and darker H3 sandstone with small elongated mud chips, overlain by a two centimetre thick fine-grained laminated sandstone (H4) grading into a silty-muddy cap – hammer for scale.

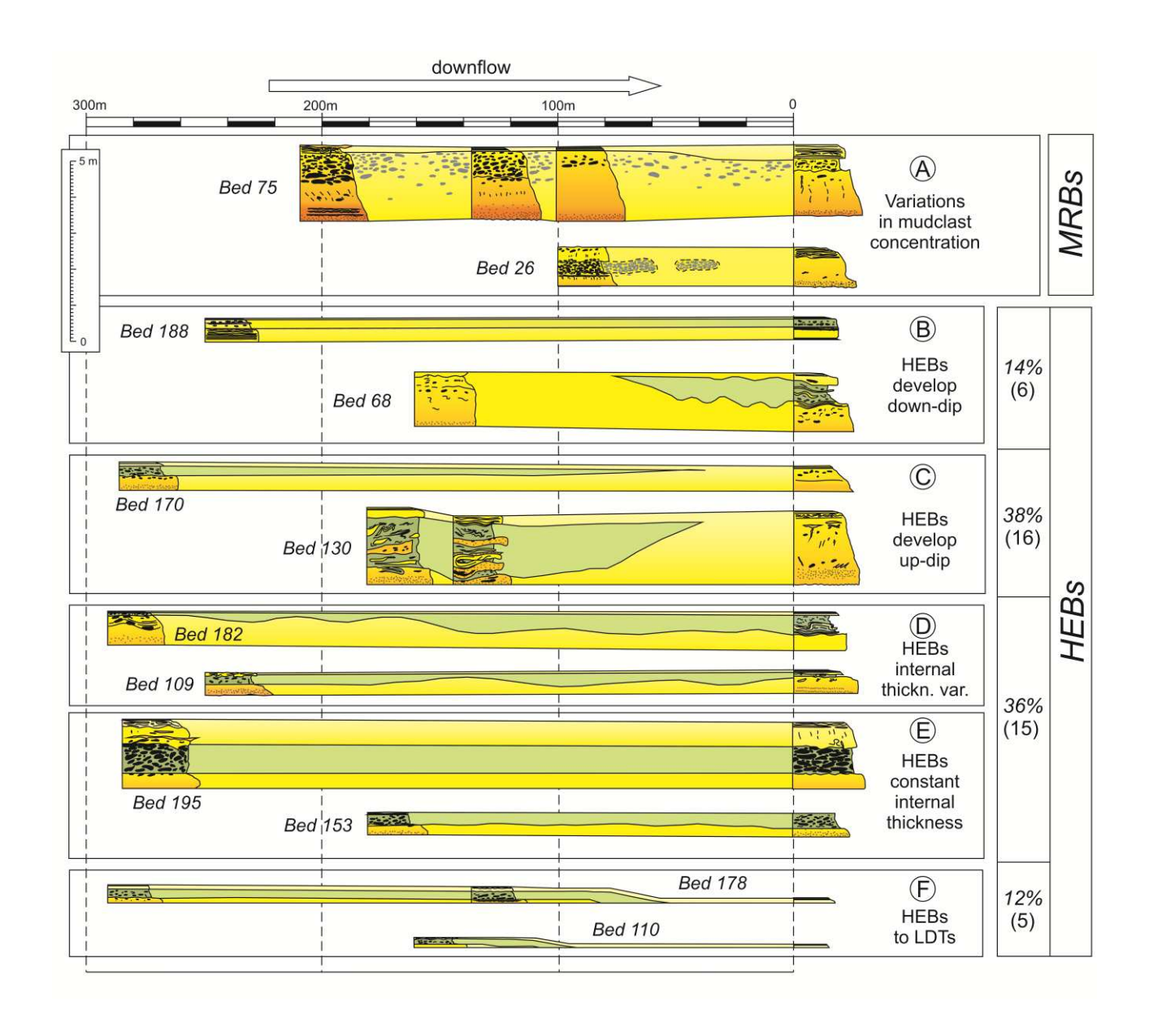


**Figure 12** – Examples of the main types of bed transitions observed in the Lago section. The values and percentages reported refer to the number of each transition type as a proportion of the total number of transitions, calculated from beds which exhibit a hybrid character in at least one of the sections. The relative position of the beds is proportional to the lateral distance between the sections; each of the recognised transition types can happen over distances between 100 and 300 metres. The database allows the scale of variability of the facies transformations to be constrained but not its wavelength, which is schematically represented in the diagram. MRBs: high-density turbidite with mudclasts.

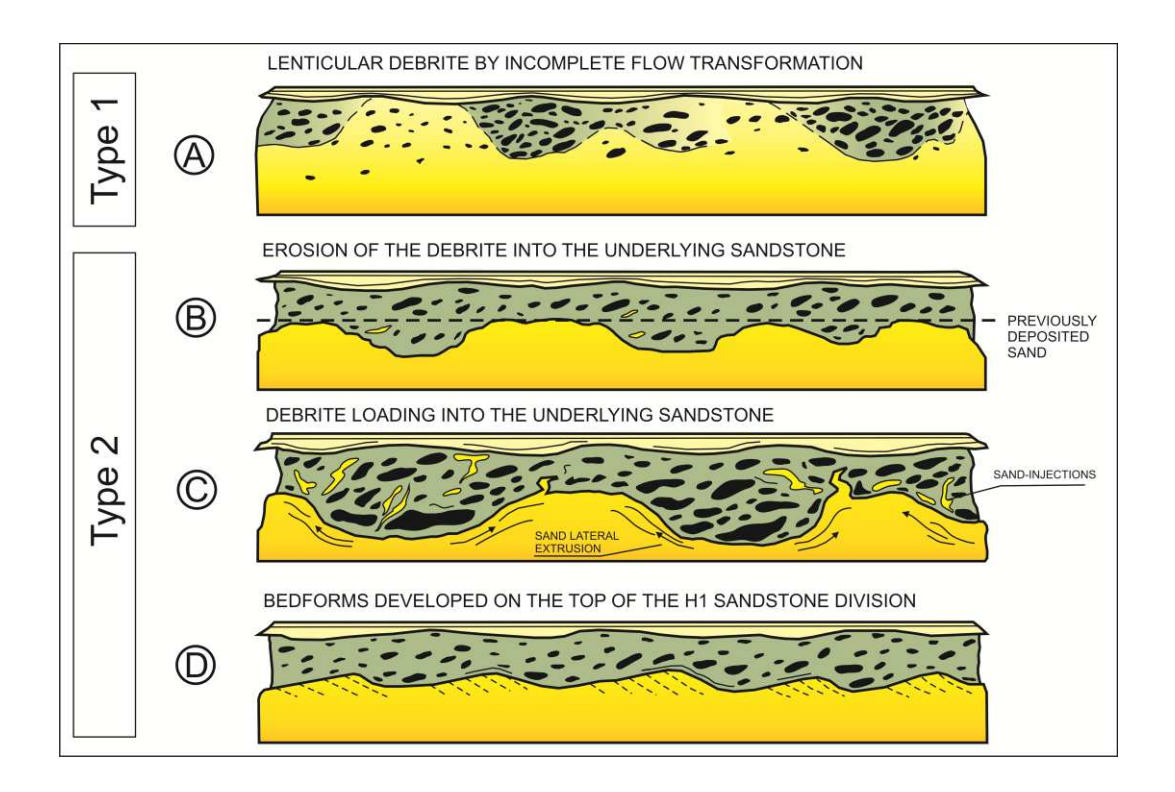


Figure 13 – Types and origin of different types of H1/H3 boundary and associated relative thickness variations: (A) short-length lateral passage (10s to 150 m) from clean sandstone with scattered mudclasts to clusters of mudclasts surrounded by muddy sandstone; (B) irregular and sharp surface separating the two divisions, and interpreted to result from erosion of the linked-debrite into a previously deposited tabular sandstone. (C) irregular and sharp surface separating the two divisions, and interpreted to result from loading of the linked-debrite and contemporaneous lateral extrusion and doming of unconsolidated basal sand producing abundant sand-injections that mix with the debrite; (D) abrupt m-scale irregularities interpreted as bedforms developed on the top of the H1 sandstone division that are then smoothed during emplacement of the overlying debrite.

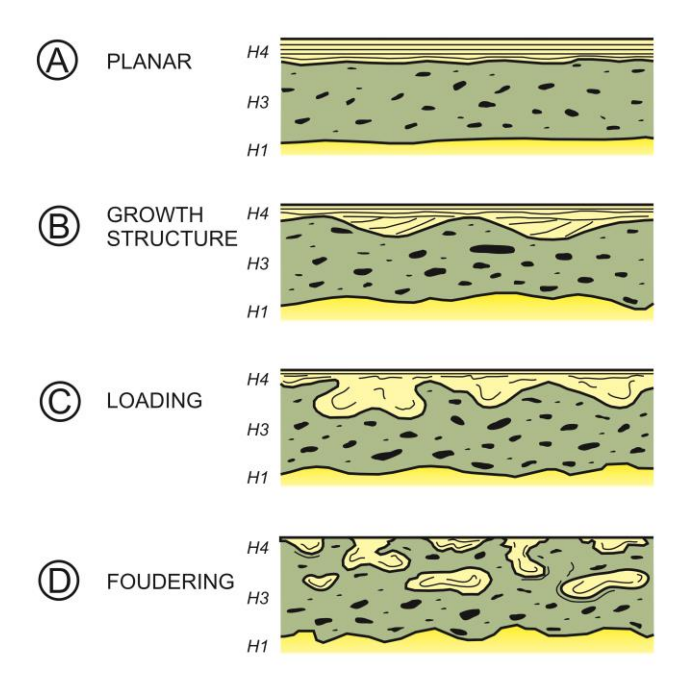
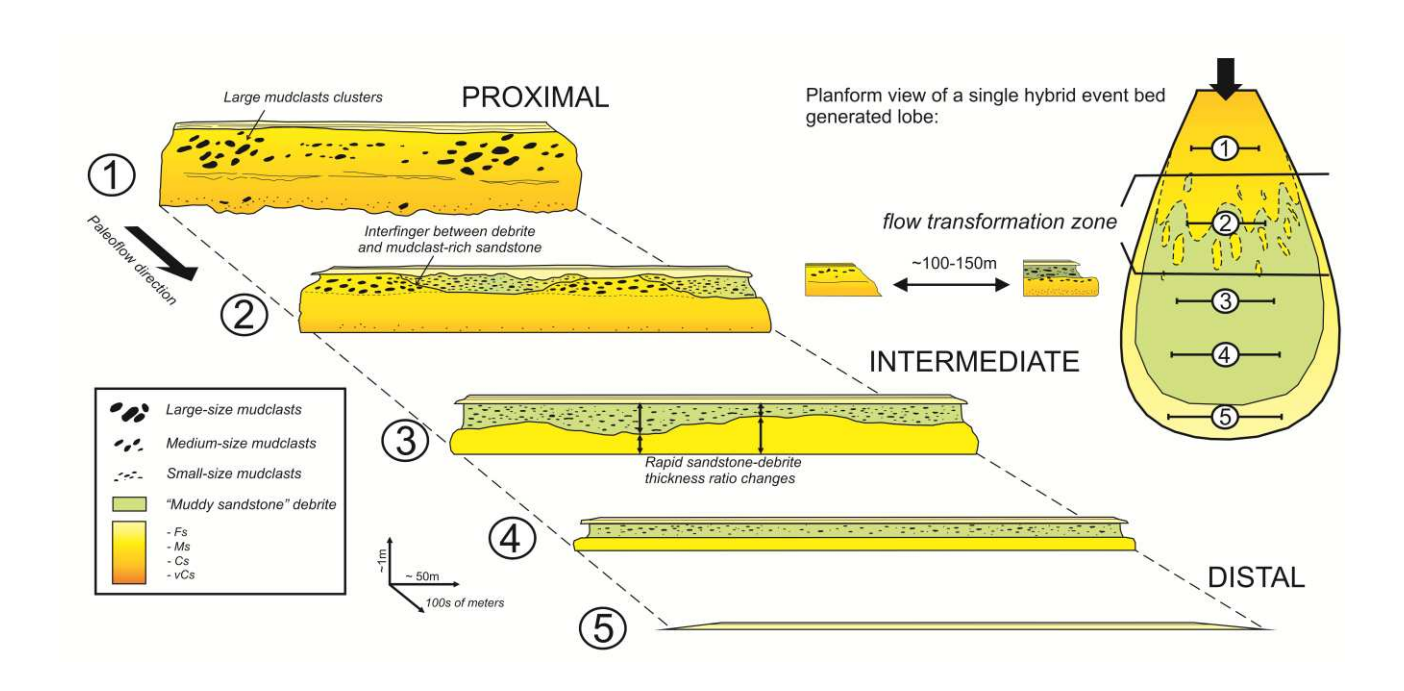
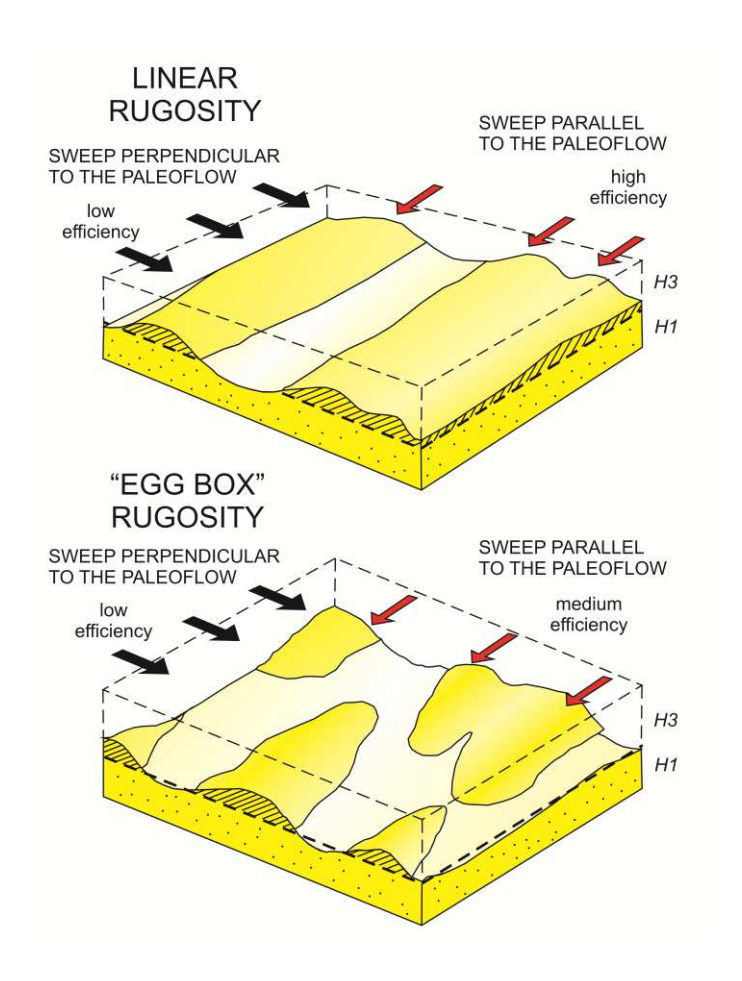


Figure 14 – Types of H3/H4 boundary with an increasing degree of linkage between the two intervals. These relationships are inferred to be controlled by the rheology of the H3 interval and by the timing of deposition from the last turbulent wake. (A) Planar contact: the H4 clean sandstone can simply cover an already flat H3 top surface without deforming it. (B) Growth structures into the underlying H3 division, which can have been either static or still moving. (C) H4 loading structures; these appear to commonly develop when the H3 division is still moving and thus can be highly deformed (e.g., Butler and McCaffrey 2010). (D) Isolated load balls/pseudonodules develop when load balls of H4 material detach and founder into H3 muddy sandstone.



**Figure 15** – Facies heterogeneity model of a single hybrid flow deposit in a series of proximal to distal lateral transects (see text for details). The rapid lateral transitions between mudclast-rich high density turbidites and fully developed hybrid event beds are shown in transect 2, and inferred to reflect complex interfingering between the up-dip sandstone and the down-dip linked-debrite. Rapid thickness variations between the basal H1 sandstone and the upper muddier debrite in laterally continuous hybrid event beds that also conserve the overall bed thickness are observed more distally – transect 3. The lobe is inferred to pass finally into a low-density turbidite facies deposited by the turbulent, more efficient tail of the gravity flow - transect 5. The dimensions and geometries provided below are drawn from the four studied examples and therefore may not span the full range of natural examples.



**Figure 16** - Linear vs. discrete ("egg box shape") end-member morphologies for the 3D expression of rugose H1/H3 contacts, and their inferred effects on internal fluid flow. The striped area represents a possible area of unswept oil at the bed scale in the low sweep efficiency case, and the dashed line the related oil-water contact; arrows indicate possible fluid circulation or interruption inside the H1 permeable sandstone. Note the sensitivity of inferred sweep efficiency to the orientation of the sweep direction (presumably up structural dip) with respect to the long axis orientation of linear rugosities – with higher efficiencies (red arrows) achieved when they align.

Table 1 - Principal geometrical, structural and sedimentological characteristics of the studied systems.

	Gottero Sandstone	Mam Tor Sandstone	Ross Sandstone	Cilento Flysch	
Location of the system	NW Apennines (Italy), Liguridi Interne, Vara Supergroup	Northern England (Uk), Pennine Basin	Western Ireland, Namurian basin	SW Apennines, Cilento Group	
Location of the outcrop	M.Ramaceto (Lorsica/Cichero)	Mam Tor quarry (Castleton)	Ballybunnion (Co. Kerry)	Lago (Castellabate)	
Age	Cretaceous- Palaeocene	Carboniferous	Carboniferous	Miocene	
Tectonic context	Trench-slope basin	Intra-cratonic basin affected by rifting	Elongated intra- cratonic basin	Piggy-back basin	
Max thickness	~1100 m	~120 m	~500 m	~2000 m	
Average paleocurrent trend	To North /Northwest	South to North	To North - Northeast	Variable (Southeast in the study interval)	
Max. lateral correlation of individual beds	Up to 4 km	Up to 240 m	Up to 70 m	Up to 290 m	
Stacking patterns in the studied area	Sheet-like and continuous thick event beds with thick mudcaps organised in 100s m cycles	Compensating outer fan lobes organised in ten mud-sand-mud cycles	Sheet-like and continuous event beds surrounded by background mudstones.	Alternation between thick sheet-like event beds and multiple bed stacks.	
Facies assoc.	Thick mudclast-rich HEBs alternate with thin LDTs (HEBs: 60%)	HEBs alternating with conventional turbidites (HDTs and LDTs) (HEBs: 41%)	Thick HEBs alternate with background mudstone (HEBs: 10%)	Thick HDTs alternated with mudclast-rich and mudclast-poor HEBs and LDTs (HEBs: 8%)	
Sub-environment	Outer fan/ basin plain	Outer fan	Basin plain	Outer fan	
References	Abbate and Sagri (1970) Casnedi (1982) Nilsen and Abbate (1984) Marini (1992, 1994)	Allen (1960) Walker (1966) Aitkenhead <i>et al.</i> (2002) Davis (2012)	Pyles and Jennette (2009) Barker (2005)	Pescatore (1966) Nardi <i>et al.</i> (2003) Cavuoto <i>et al.</i> (2007)	

**Table 2** – Lago section transitions matrix representing the number of times each bed type correlates with another in the downstream section. Self-correlations are indicated in grey. HDTs; high-density turbidites; LDTs: low-density turbidites; MRBs: high-density turbidite with mudclasts; HEBs: hybrid event beds.

	Section A (Road) - distal							
Section B (Beach) -	Bed types		HDTs	LDTs	MRBs	HEBs		
proximal		N° of correlated beds for section (total beds)	71 (82)	97 (174)	51 (55)	21 (22)		
	HDTs	49 (60)	33	5	11	0		
	LDTs	94 (259)	6	86	1	0		
	MRBs	62 (66)	23	1	32	6 (14%)		
	HEBs	36 (40)	9 (21%)	5 (12%)	7 (17%)	15 (36%)		